

1 **TITLE:**

2 **Automated Spatially Targeted Optical Micro Proteomics (autoSTOMP) to determine protein**
3 **complexity of subcellular structures**

4
5 **AUTHORS AND AFFILIATIONS:**

6 Bocheng Yin [†], Roberto Mendez[‡], Xiaoyu Zhao[†], Rishi Rahkit[‡], Ku-Lung Hsu[‡], Sarah E Ewald^{*†}

7 [†]Department of Microbiology, Immunology and Cancer Biology and the Carter Immunology
8 Center, University of Virginia School of Medicine Charlottesville VA, USA

9 [‡]Department of Chemistry, University of Virginia, Charlottesville, VA, USA

10 ^{*}Mitokinin Inc, 953 Indiana St, San Francisco, CA

11
12
13 **ABSTRACT:**

14 Spatially Targeted Optical Micro Proteomics (STOMP) is a method to study region-specific
15 protein complexity of a biological specimen. STOMP uses a confocal microscope to both visualize
16 structures of interest and to tag the proteins within those structures by a photo-driven crosslinking
17 reaction so that they can be affinity purified and identified by mass spectrometry¹. STOMP has
18 the potential to perform discovery proteomics on sub-cellular structures in a wide range of primary
19 cells types and biopsy-scale tissue samples. However, two significant limitations have prevented
20 the broad adoption of this technique by the scientific community. First, STOMP is performed
21 across two software platforms written in different languages, which requires user operation at
22 each field of view. Up to 48 hours of microscope time is necessary to tag sufficient protein (~1 µg)
23 for mass spectrometry making STOMP prohibitively time and labor-consuming for many
24 researchers. Second, the original STOMP protocol uses a custom photo-crosslinker that limits the
25 accessibility of the technique for some user. To liberate the user, we developed a protocol that
26 automates communication between Zeiss Zen Black imaging software and FIJI image processing
27 software using a customizable code in SikuliX. To fully automate STOMP (autoSTOMP), this
28 protocol includes a tool to make tile array, autofocus and capture images of fields of view across
29 the sample; as well as a method to modify the file that guides photo-tagging so that subsets of
30 the structures of interest can be targeted. To make this protocol broadly accessible, we
31 implemented a commercially available biotin-benzophenone crosslinker as well as a procedure
32 to block endogenous biotin and purify tagged proteins using magnetic streptavidin beads. Here
33 we demonstrate that autoSTOMP can efficiently label, purify and identify proteins that belong to
34 structures measuring 1-2 µm in diameter using human foreskin fibroblasts or mouse bone
35 marrow-derived dendritic cells infected with the protozoan parasite *Toxoplasma gondii* (*Tg*). The
36 autoSTOMP platform can easily be adapted to address a range of research questions using Zeiss
37 Zen Black microscopy systems and LC-MS protocols that are standard in many institutional
38 research cores.

39
40 **INTRODUCTION:**

41 Localization is a critical regulatory component of protein function. Currently, there is a
42 tremendous demand for biochemical and microscopy techniques to assess regional protein
43 complexity and function in tissues, cells, and organelles. Spatially targeted optical micro
44 proteomics (STOMP) was designed to identify the proteome of regional structures.¹ STOMP was
45 first implemented to identify components of amyloid plaques in brain sections from a mouse model
46 of prion disease and Alzheimer's disease patients.¹ In STOMP, structures of interest (SOI) are
47 stained for fluorescence microscopy and identified by confocal imaging. Confocal images are
48 used to generate a "MAP" file. Using a custom macro, the "MAP" file guides the 2-photon laser to
49 revisit structures of interest and conjugate bifunctional, UV-activated affinity purification tags to
50 proteins within those structures. The tagged proteins are affinity-purified for identification by liquid
51 chromatography-mass spectrometry (LC-MS). STOMP can be performed on a wide range of SOI

52 where one or more labeling reagents (e.g., antibodies, stains) are available to visualize it². This
53 makes STOMP well suited to perform discovery proteomics on sub-cellular structures in a wide
54 range of primary cells types and biopsy-scale tissue samples.

55 Proximity biotinylation methods like BioID and APEX, require a biotin-targeting protein that
56 is genetically engineered and stably expressed in a cell, so these tools are largely limited to cell
57 lines or cells that can be easily transduced.² In comparison, STOMP can be performed on a wider
58 range of structures of primary cells and tissues. In proximity biotinylation, regional selectivity can
59 be mediated by expressing the biotinylation enzyme on a specific side of a membrane-spanning
60 protein (e.g., PPOX, the mitochondrial matrix protein), by changing the length of the enzyme-
61 linker domain or by changing the duration of the biotinylation reaction.³ However, if there is more
62 than one pool of the label-targeting protein in the cell (e.g., ER and plasma membrane), all
63 neighboring proteins will be labeled. In comparison, STOMP uses a microscope image to guide
64 tagging, so the user has the potential to customize the photo-crosslinking coordinates to select
65 only one pool for labeling. For example, by dilating, eroding, or finding the edges of an SOI, protein
66 belonging to the core structure or near-neighbor structures can be identified. Alternatively, co-
67 localization stains can be used to identify and tag the subpopulations of the SOI. In this way,
68 region-specific SOI proteomes can be determined to inform hypotheses about the biology
69 regulated by candidate proteins. In antibody-mediated proximity biotinylation (e.g., SPPLAT or
70 BAR) a labeling enzyme is attached to an antibody specific to a protein of interest; this facilitates
71 investigating a wide range of biological specimens at a 10-100 nm resolution similar to APEX or
72 BioID.^{2,4} However, its regional selectivity is limited compared to STOMP. Laser capture
73 microdissection is often used to isolate intact cells for omics analysis.⁵ Like STOMP laser capture
74 microdissection provides a high degree of spatial selectivity. However, it is a tedious process with
75 limited resolution beyond 10 μm compared to STOMP which approaches 1 μm resolution.^{1,5}

76 The original STOMP protocol took advantage of a bi-functional 6-HIS-benzophenone
77 crosslinker for UV-mediated SOI protein tagging. The benzophenone moiety attacks any local
78 carbon or nitrogen upon exposure to UV-wavelength light. The HIS tag was implemented because
79 it could be synthesized in a cost-efficient way and benzophenone-HIS proteins were easily eluted
80 from nickel agarose columns. However, a chemical treatment of the sample with diethyl
81 pyrocarbonate (DEPC) was necessary to reduce background binding of endogenous histidine to
82 the nickel agarose matrix. A limitation of this strategy was that atypical histidine modification by
83 DEPC could negatively impact the identification of some peptides by LC-MS analysis⁶⁷. Moreover,
84 researchers that did not have access to peptide synthesis tools may not have been able to easily
85 access the 6-HIS-benzophenone reagent to perform STOMP.

86 A second major shortcoming of the original STOMP protocol was that the user must
87 manually process images in Zeiss Zen black and FIJI at each field of view. Approximately 48
88 hours of laser time were required to tag sufficient protein (1-2 μg) for MS analysis. Depending on
89 the size of the SOI, this required a user to operate the programs every 20-90 minutes for the
90 duration of the photo-labeling process¹. The benefits of this approach were that it provided
91 tremendous flexibility in selecting biotinylation targets, and it allowed the user to assess each
92 image for staining artifacts. However, extensive user intervention also introduced the opportunity
93 for user error or experimental variability.

94 Our goal was to develop a fully automated protocol for STOMP using commercially
95 available reagents and an intuitive user interface that could be implemented using hardware
96 standard in many labs and research cores. We refer to this protocol as automated STOMP
97 (autoSTOMP). To communicate between Zeiss Zen Black and FIJI software, we used the open-
98 source, icon recognition software SikuliX (<http://sikulix.com>). SikuliX is written in the Jython
99 (<https://www.jython.org>) language and can be easily coded in by users without extensive
100 programming skills. The autoSTOMP protocol integrates an autofocus and tile array platform that
101 eliminates the need for time-consuming user intervention. Finally, we implemented a new
102 biochemistry protocol using biotin-benzophenone that includes steps to block endogenous biotin

103 and streptavidin-precipitation enrichment of biotinylated proteins. To validate the specificity of
104 autoSTMOP laser targeting and biotinylated protein enrichment we infected human or murine
105 cells with the protozoan parasite *Toxoplasma gondii* (*Tg*).⁸⁻¹⁰ *Tg* has a diverse proteome of over
106 6,000 predicted protein-coding genes that are differentially expressed across three parasite life
107 stages. Protozoa diverged from the common mammalian ancestor approximately 2 billion years
108 ago, so the *Tg* proteome is sufficiently distinct from mouse and human proteomes to facilitate
109 peptide alignment for the majority of proteins. These proof of principle experiments establish
110 autoSTMOP as a robust and reproducible protocol to identify regional proteomes in biological
111 samples.

112 **MATERIALS AND METHODS:**

113 **Reagents and consumables**

114 Unless otherwise noted chemical reagents and consumables were purchased from
115 Thermo Fisher Scientific, USA, and used according to manufacturer instructions.

116 ***Tg* infections and immunofluorescence staining**

117 *Tg* is cultured and stored under BSL2 conditions in accordance with the University of
118 Virginia Environmental Health and Safety approved Biosafety Protocol. The Type II *Tg* parasite
119 strain ME49 was used in all experiments. *Tg* was passaged in confluent human foreskin
120 fibroblasts (HFF) grown in 25cm² tissue culture flasks. Parasites and HFFs were cultured in
121 complete DMEM media containing DMEM (11965118), 10% heat-shocked FBS (12303C-500ML,
122 Sigma Aldrich), 1% Penicillin/Streptomycin solution (15140163, Fisher Scientific), 1% L-glutamine
123 solution (25030164, Fisher Scientific), and 1% 100 mM sodium pyruvate solution (11360070, Life
124 Technologies), 1% 1 M HEPES solution (15630080, Life Technologies). Media was stored at 4
125 °C and warmed to 37 °C before use. C57BL/6 mice were bred in the University of Virginia vivarium
126 in accordance with ABSL-1 standards and AALAC approved protocol. Mouse bone marrow-
127 derived dendritic cells (mBMDCs) were differentiated for 6-8 days in complete RPMI media
128 supplemented with 10% mouse GMCSF supernatant derived from B16 cells stably expressing
129 mouse GMCSF as previously described⁸. THP-1 cells were cultured in suspension in complete
130 RPMI media containing RPMI (10-040-CV, Corning), 10% heat-shocked FBS, 1%
131 Penicillin/Streptomycin solution, 1% L-glutamine solution, and 1% 100 mM sodium pyruvate
132 solution, 1% 1 M HEPES.

133 For experimental infections, 0.5x10⁶ THP-1 cells were differentiated with complete RPMI
134 media containing 100 ng/mL PMA (AAJ63916MCR, Fisher Scientific) for 2 days on 12 mm cover
135 glass (64-0712, Harvard Apparatus, USA) coated with poly-D-lysine (ICN15017550). mBMDCs
136 were plated 1.35x10⁶ per well of a 12 well plate containing a single 18 mm round cover glass (64-
137 0714, Harvard Apparatus, USA) coated with poly-D-lysine. HFFs were grown to confluency on
138 18mm round cover glass. *Tg* was grown in HFFs until large intracellular parasite vacuoles were
139 observed. Intracellular *Tg* was harvested by scraping infected HFF monolayers with a rubber
140 policeman and syringe lysing the HFFs through a 25G blunt-ended syringe. *Tg* was counted on a
141 hemocytometer and added to host cells at a multiplicity of infection (MOI) of 10, or for HFF
142 infections, 8.8x10⁴ parasites per mm². The *Tg* infected HFFs on coverslips were harvested after
143 2 hours.

144 **Slide Preparation for STOMP**

145 Coverslips were fixed with 100% methanol at -20 to -30 °C (prechilled) for 15 min.
146 Methanol was decanted and samples were washed three times with room temperature PBS. If
147 staining did not take place immediately, PBS was aspirated and coverslips were stored at -30 °C.
148 To stain *Tg*, the slides were blocked with 2% BSA in TBS at room temperature for 1 hour, a rabbit
149 polyclonal antibody specific to soluble tachyzoite antigen (STAG) directly conjugated to FITC
150

154 (PA1-7253, Invitrogen) was diluted 1:300 in TBS-T (0.1% Tween20) and coverslips were stained
155 at room temperature for 1 hour. Slides were washed three times with TBST. Endogenous biotin
156 was blocked with Avidin/Biotin Blocking Kit (SP-2001, Vector Laboratories) following the
157 manufacturer's protocol. The stock solution of 0.5 M biotin-dPEG@3-benzophenone (biotin-BP,
158 10267, Quanta BioDesign) in anhydrous DMSO (89139-666, VWR) is stable for 12 months when
159 stored with desiccant in the dark at -30 °C. The biotin-BP mounting media must be prepared fresh
160 (used within 4 hours) by diluting the biotin-BP stock solution in 50/50 (v/v) DMSO/water to a
161 working concentration of 1 mM biotin-BP. Coverslips were mounted in 12 µL biotin-BP mounting
162 media in a cold room (4 °C) with weak light and sealed with nail polish (Insta-Dri Fast Dry Nail and
163 Double Duty Base and Topcoat, Sally Hansen). If multiple slides were necessary, coverslips were
164 mounted the day of crosslinking and stored in the dark at room temperature before microscopy.
165

166 **Validation of biotin-benzophenone cross-linking by microscopy**

167 Following biotin-BP cross-linking, each coverslip was soaked in DI water (RT, dark) for 30
168 minutes and the nail polish seal was gently pulled away. Excess mounting media was removed
169 by three washes with 50/50 (v/v) DMSO/water followed by three washes with Mili-Q water. Slides
170 were incubated in TBST (0.1% Tween20) containing 1: 500 dilution Alexa Fluor® 594 Streptavidin
171 (#016-580-084, Jackson ImmunoResearch Lab) for 45 min. Coverslips were washed three times
172 in TBST (0.1% Tween20) and mounted with mounting media containing DAPI (H-1000, Vector
173 Laboratories) for imaging.
174

175 **Image acquisition, mask generation and UV-biotinylation using autoSTOMP**

176 All microscopy and cross-linking were performed on an LSM880 confocal microscope
177 (Carl Zeiss, Inc., Germany) and a Chameleon multiphoton light source (Coherent Inc., USA) in
178 the Ewald Lab at the University of Virginia. Images were acquired using Zen Black (Carl Zeiss).
179 Image modification and MAP file generation were performed in FIJI (FIJI Is Just ImageJ)¹¹.
180 Structures of Interest (SOI, *T_g* here) were visualized using the 25x oil emersion lens (LD LCI Plan-
181 Achromat 25x/0.81 mm Korr DIC M27) with immersion oil (518 F for 30°C, refractive index =
182 1.518, 444970-9000-000, Carl Zeiss) and the argon laser source (488 nm) with 500-530 nm
183 bandwidth. A 512 x 512 pixel² image was acquired for each field of view. Sikulix version 1.1.4
184 (<http://sikulix.com/>) was used to automate tasks between software platforms. Python (version 3.6,
185 www.python.org) and Spyder (version 3.2.8, www.spyder-ide.org) were used to generate a tile
186 array across the slide surface (~ 500 tiles). Initial images acquired by the autofocus function were
187 compared to manually acquired images to validate the signal to noise ratio. Using the Sikulix
188 automation platform, each field of view was processed as follows. First, the SOI in each field of
189 view were imaged. The .czi file was exported into FIJI where a binary image was created,
190 thresholded and/or “erode”, “dilate” or “find edges” functions were used to create a “MAP file” of
191 the regions to be photo cross-linked. The MAP file is converted to a .txt file which is imported by
192 the STOMP macro in Zen Black. In Zen Black, the STOMP macro directs the Chameleon to deliver
193 720nm light to each pixel defined in the MAP file. Cross-linking four to five million pixels typically
194 labeled sufficient protein (approximately 1 µg) for mass spectrometry analysis. A step-by-step
195 tutorial of the autoSTOMP protocol and all the source codes are deposited at GitHub (GitHub
196 Inc.).

197 [https://github.com/boris2008/Sikulix-automates-a-workflow-performed-in-multiple-software-](https://github.com/boris2008/Sikulix-automates-a-workflow-performed-in-multiple-software-platforms-in-Windows.git)
198 [platforms-in-Windows.git](https://github.com/boris2008/Sikulix-automates-a-workflow-performed-in-multiple-software-platforms-in-Windows.git)
199

200 **Streptavidin precipitation**

201 Once the UV-cross linking is complete for each slide, the coverslip was soaked in DI water
202 (RT, dark) for 30 min and the nail polish seal was gently pulled away. Excess mounting media
203 was eliminated by three washes with 50/50 (v/v) DMSO/water followed by three washes with Mili-
204 Q water. Excess water was aspirated and the coverslip was stored at -30 °C while photo-

205 crosslinking was performed on additional slides.

206 Our purification protocol for Mass Spectrometry (MS) analysis is modified from *Hadley et*
207 *al.* 2015¹. Samples are dissociated from the coverslip in 8 M urea lysis buffer containing 100 mM
208 NaCl, 25 mM Tris, 2% SDS, 0.1% tween 20, 2 mM EDTA, 0.2 mM PMSF, and 1x Roche cComplete
209 Protease inhibitor tablets (11873580001), benzonase (E1014-25KU), RNase A from bovine
210 pancreas (10109142001). Coverslips were placed on a parafilm (Bemis) membrane with cells
211 facing up and incubated with 50 μ L urea lysis buffer at room temperature for 30 min. The coverslip
212 was then rinsed with 100 μ L Mili-Q water and followed by another incubation with 50 μ L urea lysis
213 buffer at room temperature for 30 min. All of the solutions after lysis were collected and combined
214 as lysate in low protein binding 1.5 mL microcentrifuge tubes. To reduce the nucleic acid-protein
215 complex formation and associated lysate viscosity, benzonase (0.1 μ L per 5×10^6 cells) was
216 added and incubated at 37 °C for 30 min followed by RNase (0.5 μ L per 5×10^6 cells) treatment
217 at 65 °C for 15 min. The lysate was cooled to room temperature and ready for affinity purification.

218 Four different buffers were used for the affinity purification: TU (50 mM Tris-Cl, 2 M urea,
219 and 150 mM NaCl at pH=7.4), TUST (50 mM Tris-Cl, 2 M urea, 150 mM NaCl, 0.1% SDS, and
220 0.1% Tween 20 at pH=7.4), TUB (0.5 mM biotin in TU buffer) and 100 mM NH_4HCO_3 buffer. The
221 volume of lysate of each sample was filled up to 1 mL with TUST. 10 μ L Pierce™ Streptavidin
222 (SA) Magnetic Beads (88817) 50% slurry was washing with 1 mL TUST once and then added to
223 the lysate and mixed by vortexing. The mixture was incubated on a rotator at room temperature
224 for 1 hour to bind the biotinylated proteins (longer incubation time is not recommended as it will
225 increase unspecific binding). The magnet (DynaMag™-2, Invitrogen) was used to pellet the SA
226 beads. To remove unspecific bound proteins, samples were washed three times with 1 mL TUST,
227 five times with 1 mL TU, 1 time with 1 mL TUB, and three times with 1 mL 100 mM NH_4HCO_3
228 buffer. After each wash, SA beads were pelleted on the magnet for 3 min and the buffer was
229 removed by pipetting while on the magnet. For each wash, the SA beads were mixed by vortexing
230 and incubated for 5 minutes before the SA beads were applied to the magnet again. After all
231 washing, the SA beads were resuspended in 100 μ L 100 mM NH_4HCO_3 buffer.

232

233 **Western blot**

234 To validate *Tg* protein enrichment by western blot, total protein content for each sample
235 was normalized using Pierce™ Micro BCA kit (#23235, Pierce). Proteins were separated by SDS-
236 PAGE using Mini Gel Tank tool kit (25977, ThermoFisher) and were transferred to PVDF
237 membrane (1704274, Bio-Rad) using Trans-Blot Turbo Transfer System (Bio-Rad). The PVDF
238 membrane was blocked in 2% milk TBST (0.1% Tween 20) solution for 1 hour at room
239 temperature followed by sequential incubation with antibody diluted in TBST (0.1% Tween 20)
240 and alternating washing with TBST (0.1% Tween 20). Streptavidin-HRP (016-030-084, Jackson
241 ImmunoResearch) was used to probe biotin. Proteins were visualized on ChemiDoc™Touch
242 imaging system (Bio-Rad) with HRP substrate (WBLUF0100, Millipore).

243

244 **Sample preparation for LC-MS**

245 After affinity purification, on-bead reduction and alkylation of SA beads were performed in
246 1 mL 25 mM NH_4HCO_3 by adding 25 μ L 10 mM DTT at room temperature for 30 min and 25 μ L
247 15 mM iodoacetamide in dark at room temperature for 1h in sequence. To quench excess
248 iodoacetamide, 25 μ L 5 mM DDT solution was added and incubated for 10 min. Trypsin/Lys-C
249 (V5072 Promega) was directly spiked into the protein lysate at a ratio of Trypsin/Protein = 1:25.
250 Digestion was continued overnight (~12 h) at 37 °C. Formic acid was added to a final concentration
251 of 1% (v/v) to stop the trypsinization. SA beads were removed by the magnet and the supernatant
252 was saved. 7.5 nmol Angiotensin/Vasoactive Standard (A9650-1MG/V0131-.1MG, Sigma) was
253 spiked into the peptide digest. The peptide digest was desalted using Pierce™ C18 Tips with
254 binding, washing (with 0.1% formic acid in water), and eluting (with 60% acetonitrile in water)
255 steps by following the manufacturer's instructions. The sample was dried completely on the

256 SpeedVac concentrator (Model: SPD131DDA-115). The peptide digest was dissolved in 21 μ L of
257 LC-MS grade water containing 0.1% formic acid (F0507-100ML, Sigma). The digest was filtered
258 with a 0.65 μ m pore-size micro-centrifuge filter before it was loaded to an HPLC auto-injection
259 sample.

260

261 Peptide mass quantification by LC-MS

262 For the initial validation of autoSTOMP, LC-MS was performed on an linear ion trap mass
263 spectrometer (Thermo Scientific LTQ, Thermo Fisher, USA) coupled with LC (LC-20AD,
264 Shimadzu, USA) in the Hsu lab at the University of Virginia. 1 μ L (5%) of the peptide digest was
265 injected to a C18 capillary column (20 cm of 5 μ m C18 (YMC*GEL) packed in 360 μ m o.d. x 75
266 μ m i.d. fused silica) and desalted with 0.05% acetic acid at a 185 nL/min for 30 min at room
267 temperature. After desalting, a gradient of acetonitrile/0.1 M formic acid was applied for 200 min:
268 solvent A (water + 0.05% acetic acid) and solvent B (80% acetonitrile + 0.05% acetic acid) were
269 applied in the order of 0% B for 5 min, 0-25% B for 111 min, 25-45% B for 35 min, 45-95% B for
270 1 min, 95% B for 7 min, 95-0% B for 6 min, 0% B for 34 min, and re-equilibration with 0% B for 10
271 min. The separation column ran at room temperature. The eluted peptides were electro-sprayed
272 into the LTQ MS, which was operated in the positive ion mode with a “top 3” data-dependent
273 acquisition method that consisted of one MS scan (m/z: 350-1800) followed by three MS/MS
274 scans of the most abundant ions recorded in the preceding MS scan. For mass assignment IP2
275 (the Integrated Proteomics Applications, Inc., USA) using the ProLuCID algorithm was used to
276 search against human protein database (<https://www.uniprot.org>) and *Tg* protein database
277 (released 41, <https://toxodb.org/toxo/>) with reversed sequence decoys. The peptide and proteins
278 were identified with false discovery rate (FDR) smaller than 1%, separately. Differences in protein
279 and peptide abundances between the samples were based on MS/MS spectral counting using
280 the COMPARE function in the IP2-Integrated Proteomics Pipeline. The resulting MS2 spectra
281 matches were assembled into protein identifications.

282 To compare protein enrichment in *Tg* with protein enrichment at the parasite vacuole
283 membrane using the “donut” MAP file function, a Thermo Electron Q Exactive HF-X mass
284 spectrometer system with an Easy Spray ion source connected to a Thermo 75 μ m x 15 cm C18
285 Easy Spray column was used at the University of Virginia Biomolecular Analysis Facility Core. 7
286 μ L (33.3%) of the extract was injected and the peptides eluted from the column by an gradient at
287 a flow rate of 0.3 μ L/min at 40 °C for more than 1 hour. Solvent A (water + 0.1% formic acid) and
288 solvent B (80% acetonitrile + 0.1% formic acid) were applied in the order of 2% B for 1.5 min, 2-
289 23% B for 51 min, 23-35% B for 10 min, 35-95% B for 1 min, and 95% B for 5 min. The nanospray
290 ion source was operated at 1.9 kV. The digest was analyzed using a Top10 method with the MS
291 scan set to 120K resolution and HCD scans set to 30K resolution. This mode of analysis produces
292 approximately 25000 MS/MS spectra of ions ranging in abundance over several orders of
293 magnitude. The data were analyzed by database searching using the Sequest search algorithm
294 deployed in Proteome Discoverer™ (Thermo Fisher Scientific Inc. USA) against Uniprot mouse
295 and *Tg* database from toxodb with reversed sequence decoys separately. Protein (FDR < 2%)
296 and peptide identification (FDR < 0.2%) were organized and summarized by Scaffold (Proteome
297 Software, Inc).

298

299 Data Analysis

300 Common contaminants listed on the MaxQuant website
301 http://www.coxdocs.org/doku.php?id=maxquant:start_downloads.htm have been identified and
302 excluded from our protein data. The proteins possess high similarity (> 90% proteins identification
303 and >80% peptide sequence coverage) between human and *Tg* protein were excluded from
304 downstream analysis using a custom python script “myBlast.py” running on the Rivanna
305 computing server (<https://arcs.virginia.edu/rivanna>) at the University of Virginia. A Student’s t-test

306 was used to perform pair-wise comparison across the three replicates of each sample with R
307 scripts in Rstudio (version 1.1.456, www.rstudio.com/) with R packages (for examples, readr, xlsx,
308 dplyr, tidyverse) and p-values for each protein was reported. Gene Ontology (GO) and KEGG
309 pathway annotation were added using David Bioinformatics Resources 6.8¹². The enriched
310 proteins and the statistical summarization were made in R scripts with the table organization and
311 statistical tool packages mentioned above. These custom scripts are deposited at GitHub (GitHub
312 Inc.) <https://github.com/boris2008/codes-for-validating-STOMP-with-MS.git>. Plots were created
313 with R package “ggplot2 and ”ggrepel” in R or GraphPad Prism (version 8.2.1).

314 315 **RESULTS AND DISCUSSION**

316 317 **Automated STOMP Workflow**

318 To establish autoSTOMP, we followed the basic procedure to stain structures of interest
319 (SOI) (Figure 1A), to capture immunofluorescence images in Zeiss Zen Black (Figure 1B); to
320 import images to FIJI and generate “MAP” binary text files (Figure 1C); and to cross-link SOI
321 proteins with 720nm light generated by the two-photon laser source using the STOMP Macro
322 developed by Hadley et al. 2014¹ (Figure 1D). In this protocol, we used a Zeiss LSM 880 confocal
323 microscope. The original STOMP protocol was implemented to identify novel components of beta-
324 amyloid plaques in mouse and human samples using a Zeiss LSM510 microscope and a 10x
325 water immersion objective with a photo-crosslinking resolution of 0.67x0.67x1.48 μm in x, y, z
326 axis respectively (Figure 1A-E).¹ To perform STOMP we used a 25x/0.81 mm LD LCI Plan-
327 Aplanachromat oil immersion lens with a theoretical resolution of 0.38x0.38x2.50 μm in the x, y, z axis
328 (based on spatial resolution equations)¹³. Several major modifications to the initial STOP protocol
329 have been implemented for autoSTOMP (Figure 1, light orange boxes). These include using a
330 commercially available Biotin-dPEG@3-benzophenone (biotin-BP) probe (in place of 6-HIS-BP)
331 and a step to block endogenous biotins after SOI staining (Figure 1F). After crosslinking is
332 complete, samples are dissolved in a urea lysis solution and streptavidin-coated magnetic beads
333 are used to enrich biotinylated proteins in place of the previously published nickel agarose column
334 (Figure 1E). On bead trypsin/LysC protease digestion is used to isolate precipitated peptides for
335 LC-MS. In addition, a tile array function was built using Python codes to identify each field of view
336 across sample, automate focus on SOI and acquire SOI images (Figure 1G). The entire protocol
337 is fully automated using the SikuliX icon recognition software (Figure 1H) to transition between
338 the fields of view (Figure 1G), Zen Black and FIJI (Figure 1B-D) without any user intervention.
339 Progress reports or errors in the automation process are automatically sent to a user Gmail
340 account so that the system can be monitored remotely (Figure 1I).

341 The photo-excitation conditions for autoSTOMP were determined experimentally on a
342 stained macrophage monolayer by modifying the laser power (P), pixel dwell time (D), and the
343 number of iterations (I). Each field of view was targeted then samples were assessed for
344 photobleaching and sample overheating (Figure S-1A). Several conditions cause noticeable
345 photo-bleaching but no overheating (Figure S-1A, red box). $P/I/D = 3/1/1$ was chosen to minimize
346 the total time necessary to photo-crosslink the sample (with optimal photobleaching and without
347 overheating, Figure S-1B). To identify the minimum concentration of biotin-BP necessary to
348 achieve robust SA-594 signal, the concentration of biotin-BP in the mounting media was titrated.
349 Thus, optimal photo-active biotinylation was selected (Figure S-2).

350 351 **AutoSTOMP selectively biotinylates SOI**

352 To determine if autoSTOMP can effectively enrich proteins from sub-cellular SOI we
353 infected human foreskin fibroblasts (HFFs) with the ME49 strain of Type II *Toxoplasma gondii* (*Tg*)
354 which forms intracellular vacuole measuring 1-6 μm (Figure 2A). After two hours of infection, the
355 coverslips were fixed and stained with an antibody raised against soluble *Tg* antigen (commonly

356 referred to as STAG) directly conjugated to FITC (α -*Tg*-488) to identify *Tg* as the SOIs (Figure
357 2B). A MAP file was generated and used to guide UV-excitation and biotinylation reaction using
358 the autoSTOMP platform (Figure 1). Following UV-crosslinking, coverslips were removed and
359 stained with streptavidin directly conjugated to Alexafluor594 (SA-594) and reimaged (Figure 2D).
360 Co-localization was confirmed by re-imaging the *Tg*-specific antibody in the 488 nm channel
361 (Figure 2E-F). Co-localization of the α -*Tg* signal and SA-594 signal confirmed the accuracy of UV
362 targeting and the efficiency of biotinylation. As expected, the α -*Tg*-488 signal was slightly
363 photobleached upon re-imaging compared to that is before UV-targeting by autoSTOMP (Figure
364 2E versus 2B). Tile imaging around the field of view identified in the MAP file (Figure 2G, dotted
365 white box) confirmed that autoSTOMP selectively biotinylated SOI identified in the MAP and did
366 not increase background SA-594 signal relative to not-targeted fields of view (Figure 2H). Based
367 on these data, we conclude that autoSTOMP efficiently targets biotin-BP conjugation to regions
368 defined as SOI by immunofluorescence imaging.

369

370 **AutoSTOMP biotinylation and precipitation procedures enrich for SOI proteins**

371 To validate the efficiency of SOI biotinylation and streptavidin purification, *Tg* infected
372 HFFs were stained and biotinylated as described in Figure 2 (Figure 3, α -*Tg* STOMP). In parallel,
373 a negative control sample was prepared and mounted in biotin-BP, but not exposed to UV-light
374 (Figure 3, Dark). After photo-crosslinking, samples were washed of excess biotin, dissociated
375 from the slide in urea lysis buffer. Half of each sample was reserved as an "INPUT" control; in the
376 other half, biotinylated proteins were enriched on streptavidin magnetic beads (Figure 3A). Both
377 α -*Tg* STOMP and Dark samples had similar amounts of *Tg* proteins in the input control (note that
378 polyclonal antibodies raised against *Tg* STAG recognize multiple parasite proteins) (Figure 3B,
379 "INPUT" columns). *Tg* proteins were only enriched in α -*Tg* STOMP SA-P samples not the Dark
380 SA-P sample (Figure 3B). In comparison, human GAPDH was detected in both INPUT samples
381 but was not enriched in either the α -*Tg* STOMP SA-P samples or the Dark SA-P sample (Figure
382 3C). Probing the blots with Streptavidin conjugated to HRP confirmed that biotinylated proteins
383 were present in the α -*Tg* STOMP samples not the Dark samples (Figure 3D). Moreover,
384 streptavidin precipitation recovered the majority of biotin signal in the α -*Tg* STOMP SA-P sample
385 relative to INPUT (Figure 3D). These results confirm that autoSTOMP effectively conjugates
386 biotin-BP to SOI proteins and that biotinylated SOI proteins are enriched by the SA-P procedure.

387

388 **AutoSTOMP enriches for SOI proteins by LC-MS**

389 We next asked if *Tg* SOI proteins could be enriched and identified by LC-MS using
390 autoSTOMP. Samples were prepared and precipitated as described in Figure 3. After precipitation,
391 peptides were digested on SA-beads with trypsin/LysC for mass spectrometry (Figure 4). For
392 each sample, approximately 1 μ g of protein was recovered for LC-MS. Peptide mass was
393 identified by ion trap mass spectrometry coupled with liquid chromatography and searched
394 against the *Tg* protein database (combined from ME49, GT1, VEG, and RH parasite strains) or
395 the human protein database. Peptides that could not be uniquely assigned to either proteome
396 database were excluded from downstream analysis of protein abundance. Proteins were
397 quantified by the number of spectral counts and ranked in order of abundance (Table S-1, Figure
398 4).

399 In total, 736 parasite proteins and 960 human proteins were detected in all samples with
400 false discovery ratio (FDR) < 1% for peptide identification and an FDR < 1% for protein
401 identification (Table S-1). The majority of *Tg* proteins identified were enriched in the α -*Tg* STOMP
402 precipitate (SA-P) sample relative to Dark SA-P samples by spectral count ratio (Figure 4A). As
403 expected, human proteins were not similarly enriched in α -*Tg* STOMP SA-P relative to dark SA-
404 P (Figure 4B). In the INPUT controls, the spectral counts ratio for most *Tg* proteins (Figure 4C)
405 and human proteins (Figure 4D) were close to 1, indicating consistent representation of proteins

406 across samples. To determine if any of the proteins identified were significantly enriched in α -*Tg*
407 STOMP relative to Dark samples we calculated the $-\log_{10}$ p-value over the log scale of ratio of
408 spectral counts of the samples (Figure 4E-H). 47.1% of the 736 *Tg* proteins were significantly
409 enriched (p-value < 0.05, a $-\log_{10}$ p-value > 1.30 and $\log_2 R > 1$) in α -*Tg* STOMP SA-P relative to
410 the Dark SA-P sample (Figure 4E, black box). By contrast, only 1.8% of the 960 human proteins
411 were significantly enriched in α -*Tg* STOMP SA-P relative to the Dark SA-P samples (Figure 4F).
412 As expected, few *Tg* proteins (Figure 4G, 1.8%) and no human proteins (Figure 4H) were
413 significantly enriched in α -*Tg* STOMP INPUT relative to and Dark INPUT controls.

414 We also examined protein enrichment based on abundance as the primary criterion. We
415 considered proteins with spectral counts ≥ 5 to be represented within a high confidence interval
416 based on the spectral count distribution model.¹⁴ Of the 69 high confidence *Tg* proteins in the
417 input control 61 (88.4%) were significantly enriched in the SA-P sample (Table S-2, sheet 1;
418 Figure S-3A-B), indicating that STOMP reliably reports the most abundant parasite proteins in the
419 sample. Of the 667 low abundance *Tg* proteins in the INPUT controls (spectral counts < 5) 149
420 were represented with high confidence in α -*Tg* STOMP SA-P samples (spectral counts ≥ 5)
421 (Figure S-3B). The 42.88% of these (Figure S-3C) were significantly enriched in the α -*Tg* STOMP
422 SA-P sample relative to Dark SA-P sample confirming that autoSTOMP also enriched low
423 confidence *Tg* proteins (Table S-2, sheet 2). The limited number of proteins with spectral counts
424 ≥ 5 is likely a function of the small sample concentration used for LC-MS analysis and the
425 sensitivity of the Thermo Scientific LTQ used in this experiment. In summary, these data indicate
426 that SOI proteins represented in a total cellular proteome at both high and low confidence can be
427 tagged and detected by autoSTOMP with high confidence.

428 **AutoSTOMP selectively enriches proteins structures adjacent to the stained targets**

430 An advantage of autoSTOMP compared to proximity-biotinylation methods is that the SOI
431 can be determined by simply modifying the MAP file.^{4,15} The region surrounding the parasite is a
432 biologically relevant organelle called the parasite vacuole membrane (PVM) that is composed of
433 host-derived lipids, secreted parasite effector proteins, as well as host proteins that regulate
434 vesicular trafficking, immune functions and organelle recruitment (including endoplasmic
435 reticulum, mitochondria and lysosomes).¹⁶ The original STOMP protocol was shown to biotinylate
436 structures measuring 1 μm by microscopy, however, the majority of β -amyloid plaques examined
437 measured between 10-50 μm in diameter.¹ We reasoned that generating a MAP file from the 1
438 μm region surrounding but excluding the parasite signal would allow us to identify candidate host
439 and parasite proteins belonging to the PVM. To do this, mouse bone marrow derived dendritic
440 cells (mBMDCs) were infected with *Tg* for two hours and samples were prepared for autoSTOMP
441 (Figure 5A). We first confirmed that *Tg* within mBMDCs were selectively and efficiently targeted
442 by autoSTOMP using the parameters defined in Figure 2 (Figure S-4, α -*Tg*-488). To target the
443 region surrounding but excluding *Tg* the SOI was defined by identifying the perimeter of the α -*Tg*-
444 488 signal (Figure 5B) and dilating the perimeter to generate a 1 μm "DONUT" outside the parasite
445 using the "donut macro" in FIJI (Figure 5C). AutoSTOMP selectively biotinylated the DONUT SOI
446 surrounding *Tg* at approximately 1 μm in the x and y axis (Figure 5D-F) within the targeted field
447 of view (Figure 5G-H).

448 Next, the DONUT SOI or Dark controls were precipitated as described in Figure 3 and
449 submitted for mass spectrometry using a high-performance Velos Orbitrap LC-MS for
450 downstream analysis (Figure 6). 138 *Tg* proteins were identified in the STOMP DONUT SA-P
451 sample (Figure 6A), 47.1% (65 proteins) of these were significantly enriched (Figure 6B). Among
452 the enriched *Tg* proteins were several secreted parasite proteins with known localization to the
453 PVM or the adjacent intravacuolar network. These included rhoptry neck protein RON2, rhoptry
454 protein ROP7, dense granule protein GRA3, microneme proteins MIC4 (Figure 6C).¹⁷⁻¹⁹ Although
455 differences in the MS protocol mean that we cannot directly compare α -*Tg* STOMP SA-P (Figure

456 4E) with STOMP DONUT SA-P (Figure 6B) it is notable that the majority of parasite proteins
457 identified within the *Tg* SOI (Table S-2) are not represented in the DONUT SOI (Table S-4),
458 consistent with the expected spatial selection of parasite proteins trafficked to the PVM.

459 2230 mouse proteins were identified in the STOMP DONUT SA-P relative to Dark SA-P
460 (Figure 6D), 72.5% of which were significantly enriched (Figure 6E). In comparison to the α -*Tg*
461 STOMP SA-P proteome in which significantly enriched parasite proteins were 19 times more
462 abundant than host proteins (Figure 4E-F), the STOMP DONUT SA-P contained 24 times the
463 number of significantly enriched host proteins compared to *Tg* proteins (Figure 6E&B). At least
464 16 of these host proteins have been detected at the PVM or the intravacuolar network during *Tg*
465 infection (Figure 6E). Ras-related protein Rab-7 and cathepsin D are associated with
466 autophagosomal formation around PVM and lysosomal fusion *Tg* clearance.^{16,20} The AP-2
467 regulates endosomal vesicle fusion with autophagosomes and the PVM.²¹ Proteins expressed in
468 the mitochondria including the V-type proton ATPase and Rab associated proteins that regulate
469 Golgi vesicular transport might also be expected based on reports of recruitment of these
470 structures to the PVM.²¹⁻²³

471 In addition to identifying host proteins that have been experimentally confirmed at the
472 PVM, we searched the significantly enriched mouse proteins against gene ontology (GO) and
473 Kyoto Encyclopedia of Genes and Genomes (KEGG) pathway annotation libraries with David
474 Bioinformatics Resources 6.8.¹² Using the GO term “biological processes”, 20.5% of STOMP
475 DONUT SA-P proteins belong to the “transport” annotation group and 7.7% are in “metabolic
476 processes” annotation group (Figure 6G) consistent with parasite scavenging from the host.²⁴
477 Using the GO term “molecular function,” 32.6% proteins are associated with “protein binding” and
478 15.3% are involved in ATP binding consistent with regulation of membrane fusion at the PVM
479 (Figure 6H).²⁵ Using the GO term cellular component, more than 55% proteins are annotated with
480 “membrane” GOCC term (Figure 6I). KEGG analysis also indicated that 18.3% of proteins belong
481 to the “metabolic pathways” annotation (Figure 6J); and proteins associated with organelles that
482 are known to be recruited to the PVM were represented including endolysosomal vesicles,
483 endoplasmic reticulum and mitochondria.^{16,25-27} Based on these data, we conclude that
484 autoSTOMP selectively enriches proteins belonging to sub-cellular regions with spatial resolution
485 of approximately 1 μ m.

486 487 **CONCLUSION**

488
489 Here we show that autoSTOMP is a fully automated platform to visualize, tag, affinity purify
490 and identify proteins by mass spectrometry. AutoSTOMP represents a significant technological
491 advance because it liberates the user from field-by-field task management previously required to
492 perform STOMP. In automating the STOMP protocol, we retained and refined the ability to define
493 regions of interest based on structure size, shape or localization using FIJI image analysis
494 software. This flexibility is a major advantage of STOMP compared to other proximity-based
495 tagging tools ^{2,4}

496
497 Our choice of a biotin-BP was based on the low background reactivity of the BP group and
498 the high affinity of the biotin-streptavidin interaction. Benzophenone covalently inserts into N-H or
499 C-H bond upon excitation with UV-wavelength light¹. However, the cost of this tagging strategy is
500 that most BP modified peptides will remain attached to the SA beads. Any eluted peptides bearing
501 biotin-BP will not be recognized by MS, due to the uncertain mass shift imparted by the tag. For
502 this reason, an ideal ratio of biotin-BP would be one tag per protein which may be optimizable in
503 future experiments.

504
505 Finally, it is important to note that autoSTOMP is not limited to host-pathogen interactions
506 as studied here. We chose this system because it took advantage of organisms with diverse and

507 divergent proteomes in extremely close proximity to one another, which allowed us to accurately
508 quantify protein enrichment in SOIs relative to background. Our data suggest that autoSTOMP
509 can be used to identify proteins belonging to 1 μ m scale sub-cellular structures in a range of
510 biological specimens.

511 ASSOCIATED CONTENT

512 Supporting Information

- 513 1. Table S-1. The *Tg* and Human proteins identified in the samples from *Tg* infected HFFs
514 related to Figure 4.
- 515 2. Table S-2. The *Tg* proteins that are filtered under two different conditions related to Figure
516 4: "INPUT > 4": proteins beyond the SC cutoff of 5 in the INPUT controls; "SA-P > 4 INPUT
517 < 4": proteins below the SC cutoff of 5 in the INPUT controls, but beyond the SC cutoff of
518 5 in the SA-P samples.
- 519 3. Table S-3. The *Tg* and mouse proteins identified in the *Tg* surrounding regions excluding
520 *Tg* in mBMDCs infected with *Tg* related to Figure 6.
- 521 4. Table S-4. The *Tg* and mouse proteins significantly enriched in the *Tg* surrounding regions
522 excluding *Tg* related to Figure 6.
- 523 5. Figure S-1. The photo-crosslinking condition was optimized at power/iteration/dwell time
524 in ms (P/I/D) = 3/1/1.
- 525 6. Figure S-2. Optimize the biotin-BP at a concentration of 1 mM for photoactive labelling.
- 526 7. Figure S-3. Half of total *Tg* proteins with either high or low abundance (confidence) in the
527 INPUT controls were enriched in α -*Tg* STOMP SA-P samples by autoSTOMP procedure
528 (related to Figure 4E).
- 529 8. Figure S-4. Validate the photo-crosslinking biotinylation on *Tg* SOIs in mBMDCs infected
530 with *Tg* with autoSTOMP.

531 AUTHOR INFORMATION

532 Corresponding Author:
533 *Phone: 434-924-1925. E-mail: se2s@virginia.edu

534 ORCID^{ID}
535 Bocheng Yin: 0000-0003-1755-2728
536 Roberto Mendez: 0000-0001-5355-112X
537 Xiaoyu Zhao: 0000-0001-5095-7212
538 Ku-Lung Hsu: 0000-0001-5620-3972
539 Sarah E. Ewald: 0000-0002-5327-7578

540 Author Contributions
541 B.Y., R.R. and S.E.E. designed the experiments in this study. X.Z. provided biological specimens
542 for these studies. B.Y. performed the STOMP experiments, data processing and analysis. R.M.
543 and K-L.H conducted Mass Spec experiments using the Thermo Scientific LTQ. B.Y. and S.E.E.
544 prepared the manuscript.

545 Notes
546 The authors declare no competing financial interest.

547 **ACKNOWLEDGMENTS:**
548 We thank Dr. Nicholas E. Sherman and Dr. Jeong-Jin Park at the W.M. Keck Biomedical
549

558 Mass Spectrometry Laboratory at the University of Virginia's School of Medicine for providing
559 Mass Spectrometry analysis service for experiments using the Velos Orbitrap. We thank Anson
560 Parker at the University of Virginia School of Medicine Library for the introduction to SikuliX. We
561 thank Dr. Hardik at the University of Virginia School of Medicine, for assistance in the design and
562 execution of the Python script to process *Tg* and human protein assignments. We thank Dr. Josh
563 Elias at The Chan Zuckerberg Institute for guidance in the design and execution of mass
564 spectrometry experiments. We are grateful to Dr. Avi Chakraborty and Dr. Kevin Hadley at the
565 University of Toronto for extensive discussion of STOMP optimization, initial training with the
566 STOMP pipeline and assistance using the STOMP Macro.

567 This work was supported by NIH K22 AI116727 (SEE) AMH/Allen Institute 31315 (SEE)
568 and start-up funds from the University of Virginia SOM and the Emily Couric Cancer Center.
569

570 DISCLOSURES:

571 The authors have nothing to disclose.
572

573

573 REFERENCES

- 574 (1) Hadley, K. C.; Rakhit, R.; Guo, H.; Sun, Y.; Jonkman, J. E. N.; McLaurin, J.; Hazrati, L.-N.;
575 Emili, A.; Chakrabarty, A. Determining Composition of Micron-Scale Protein Deposits in
576 Neurodegenerative Disease by Spatially Targeted Optical Microproteomics. *Elife* **2015**, *4*,
577 e09579. <https://doi.org/10.7554/eLife.09579>.
- 578 (2) Chen, C.-L.; Perrimon, N. Proximity-Dependent Labeling Methods for Proteomic Profiling
579 in Living Cells. *Wiley Interdiscip. Rev. Dev. Biol.* **2017**, *6* (4), 10.1002/wdev.272.
580 <https://doi.org/10.1002/wdev.272>.
- 581 (3) Rhee, H.-W.; Zou, P.; Udeshi, N. D.; Martell, J. D.; Mootha, V. K.; Carr, S. A.; Ting, A. Y.
582 Proteomic Mapping of Mitochondria in Living Cells via Spatially Restricted Enzymatic
583 Tagging. *Science* (80-.). **2013**, *339* (6125), 1328 LP – 1331.
584 <https://doi.org/10.1126/science.1230593>.
- 585 (4) Bar, D. Z.; Atkatsch, K.; Tavarez, U.; Erdos, M. R.; Gruenbaum, Y.; Collins, F. S.
586 Biotinylation by Antibody Recognition—a Method for Proximity Labeling. *Nat. Methods*
587 **2017**, *15*, 127.
588 <https://doi.org/10.1038/nmeth.4533>[https://www.nature.com/articles/nmeth.4533#supplem](https://www.nature.com/articles/nmeth.4533#supplementary-information)
589 [entary-information](https://www.nature.com/articles/nmeth.4533#supplementary-information).
- 590 (5) Espina, V.; Wulfschlegel, J. D.; Calvert, V. S.; VanMeter, A.; Zhou, W.; Coukos, G.; Geho, D.
591 H.; Petricoin, E. F.; Liotta, L. A. Laser-Capture Microdissection. *Nat. Protoc.* **2006**, *1* (2),
592 586–603. <https://doi.org/10.1038/nprot.2006.85>.
- 593 (6) Wallis, R. B.; Holbrook, J. J. The Reaction of a Histidine Residue in Glutamate
594 Dehydrogenase with Diethyl Pyrocarbonate. *Biochem. J.* **1973**, *133* (1), 183–187.
595 <https://doi.org/10.1042/bj1330183>.
- 596 (7) Kim, M.-S.; Zhong, J.; Pandey, A. Common Errors in Mass Spectrometry-Based Analysis
597 of Post-Translational Modifications. *Proteomics* **2016**, *16* (5), 700–714.
598 <https://doi.org/10.1002/pmic.201500355>.
- 599 (8) Ewald, S. E.; Chavarria-Smith, J.; Boothroyd, J. C. NLRP1 Is an Inflammasome Sensor for
600 *Toxoplasma Gondii*. *Infect. Immun.* **2014**, *82* (1), 460–468.
601 <https://doi.org/10.1128/IAI.01170-13>.
- 602 (9) Hatter, J. A.; Kouche, Y. M.; Melchor, S. J.; Ng, K.; Bouley, D. M.; Boothroyd, J. C.; Ewald,
603 S. E. *Toxoplasma Gondii* Infection Triggers Chronic Cachexia and Sustained Commensal
604 Dysbiosis in Mice. *PLoS One* **2018**, *13* (10), e0204895.
605 <https://doi.org/10.1371/journal.pone.0204895>.
- 606 (10) Coppens, I. Exploitation of Auxotrophies and Metabolic Defects in *Toxoplasma* as
607 Therapeutic Approaches. *Int J Parasitol* **2014**, *44* (2), 109–120.
608 <https://doi.org/10.1016/j.ijpara.2013.09.003>.

- 609 (11) Schindelin, J.; Arganda-Carreras, I.; Frise, E.; Kaynig, V.; Longair, M.; Pietzsch, T.;
610 Preibisch, S.; Rueden, C.; Saalfeld, S.; Schmid, B.; et al. Fiji - an Open Source Platform
611 for Biological Image Analysis. *Nat. Methods* **2012**, *9* (7), 10.1038/nmeth.2019.
612 <https://doi.org/10.1038/nmeth.2019>.
- 613 (12) Huang, D. W.; Sherman, B. T.; Lempicki, R. A. Systematic and Integrative Analysis of Large
614 Gene Lists Using DAVID Bioinformatics Resources. *Nat. Protoc.* **2009**, *4* (1), 44–57.
615 <https://doi.org/10.1038/nprot.2008.211>.
- 616 (13) Benninger, R. K. P.; Piston, D. W. Two-Photon Excitation Microscopy for the Study of Living
617 Cells and Tissues. *Curr. Protoc. cell Biol.* **2013**, *Chapter 4*, Unit-4.11.24.
618 <https://doi.org/10.1002/0471143030.cb0411s59>.
- 619 (14) Choi, H.; Larsen, B.; Lin, Z. Y.; Breitkreutz, A.; Mellacheruvu, D.; Fermin, D.; Qin, Z. S.;
620 Tyers, M.; Gingras, A. C.; Nesvizhskii, A. I. SAINT: Probabilistic Scoring of Affinity
621 Purification-Mass Spectrometry Data. *Nat. Methods* **2011**, *8* (1), 70–73.
622 <https://doi.org/10.1038/nmeth.1541>.
- 623 (15) Rhee, H.; Zou, P.; Udeshi, N. D.; Martell, J. D.; Mootha, V. K.; Carr, S. A.; Ting, A. Y.
624 Proteomic Mapping of Mitochondria. *Science (80-.)*. **2013**, *339* (March), 1328.
625 <https://doi.org/10.1126/science.1230593>.
- 626 (16) Clough, B.; Frickel, E.-M. M. The Toxoplasma Parasitophorous Vacuole: An Evolving
627 Host–Parasite Frontier. *Trends Parasitol.* **2017**, *33* (6), 473–488.
628 <https://doi.org/10.1016/j.pt.2017.02.007>.
- 629 (17) Besteiro, S.; Michelin, A.; Poncet, J.; Dubremetz, J. F.; Lebrun, M. Export of a Toxoplasma
630 Gondii Rhopty Neck Protein Complex at the Host Cell Membrane to Form the Moving
631 Junction during Invasion. *PLoS Pathog.* **2009**, *5* (2).
632 <https://doi.org/10.1371/journal.ppat.1000309>.
- 633 (18) Dunn, J. D.; Ravindran, S.; Kim, S. K.; Boothroyd, J. C. The Toxoplasma Gondii Dense
634 Granule Protein GRA7 Is Phosphorylated upon Invasion and Forms an Unexpected
635 Association with the Rhopty Proteins ROP2 and ROP4. *Infect. Immun.* **2008**, *76* (12),
636 5853–5861. <https://doi.org/10.1128/IAI.01667-07>.
- 637 (19) Camejo, A.; Gold, D. A.; Lu, D.; McFetridge, K.; Julien, L.; Yang, N.; Jensen, K. D. C.; Saeij,
638 J. P. J. Identification of Three Novel Toxoplasma Gondii Rhopty Proteins. *Int. J. Parasitol.*
639 **2014**, *44* (2), 147–160. <https://doi.org/10.1016/j.ijpara.2013.08.002>.
- 640 (20) Stoka, V.; Turk, V.; Turk, B. Lysosomal Cathepsins and Their Regulation in Aging and
641 Neurodegeneration. *Ageing Res. Rev.* **2016**, *32*, 22–37.
642 <https://doi.org/10.1016/j.arr.2016.04.010>.
- 643 (21) Luzio, J. P.; Hackmann, Y.; Dieckmann, N. M. G.; Griffiths, G. M. The Biogenesis of
644 Lysosomes and Lysosome-Related Organelles. *Cold Spring Harb. Perspect. Biol.* **2014**, *6*
645 (9). <https://doi.org/10.1101/cshperspect.a016840>.
- 646 (22) Nakano, R.; Ohira, M.; Yano, T.; Imaoka, Y.; Tanaka, Y.; Ohdan, H. Hepatic Irradiation
647 Persistently Eliminates Liver Resident NK Cells. *PLoS One* **2018**, *13* (6), 1–16.
648 <https://doi.org/10.1371/journal.pone.0198904>.
- 649 (23) Kelly, F. D.; Wei, B. M.; Cygan, A. M.; Parker, M. L.; Boulanger, M. J.; Boothroyd, J. C.
650 Toxoplasma Gondii MAF1b Binds the Host Cell MIB Complex To Mediate Mitochondrial
651 Association. *mSphere* **2017**, *2* (3). <https://doi.org/10.1128/mSphere.00183-17>.
- 652 (24) Blume, M.; Seeber, F. Metabolic Interactions between Toxoplasma Gondii and Its Host.
653 *F1000Research* **2018**, *7* (0), 1–10. <https://doi.org/10.12688/f1000research.16021.1>.
- 654 (25) Håkansson, S.; Charron, A. J.; Sibley, L. D. Toxoplasma Evacuoles: A Two-Step Process
655 of Secretion and Fusion Forms the Parasitophorous Vacuole. *EMBO J.* **2001**, *20* (12),
656 3132–3144. <https://doi.org/10.1093/emboj/20.12.3132>.
- 657 (26) Sinai, A. P.; Webster, P.; Joiner, K. A. Association of Host Cell Endoplasmic Reticulum and
658 Mitochondria with the Toxoplasma Gondii Parasitophorous Vacuole Membrane: A High
659 Affinity Interaction. *J. Cell Sci.* **1997**, *110* (17), 2117–2128.

660 (27) Pernas, L.; Adomako-Ankomah, Y.; Shastri, A. J.; Ewald, S. E.; Treeck, M.; Boyle, J. P.;
661 Boothroyd, J. C. Toxoplasma Effector MAF1 Mediates Recruitment of Host Mitochondria
662 and Impacts the Host Response. *PLoS Biol.* **2014**, *12* (4).
663 <https://doi.org/10.1371/journal.pbio.1001845>.
664

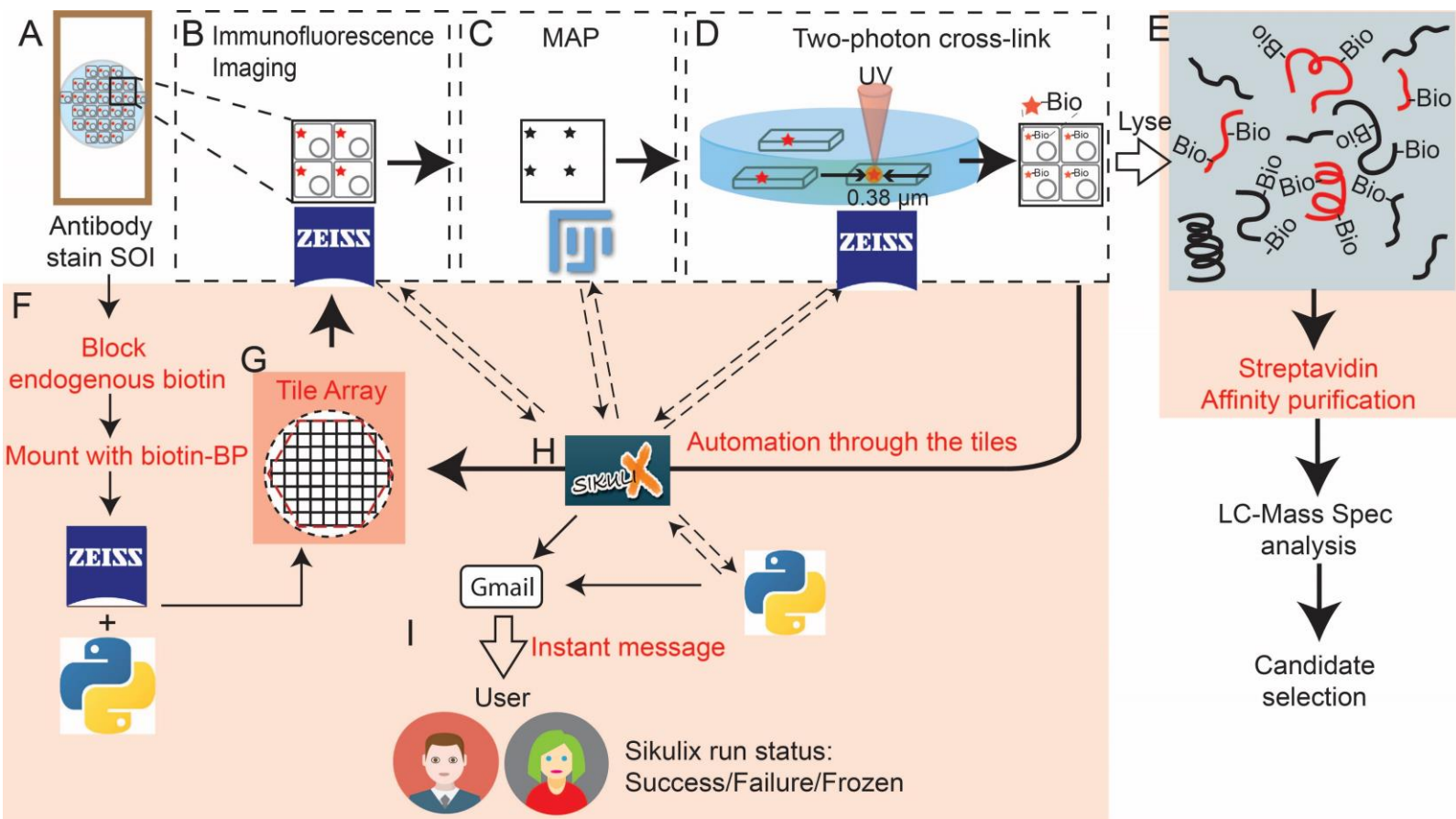


Figure 1. Overview of the Spatially Targeted Optical Micro Proteomics (STOMP) protocol (A-D) and automated-STOMP modification (E-I, orange boxes). **A**, Structures of interest (SOI) are stained for identification by standard fluorescence microscopy. **B**, SOI are identified by immunofluorescence imaging in visible (non-UV) wavelengths using Zeiss Zen Black software. **C**, Immunofluorescence images are exported to FIJI software used to generate a “map” file. **D**, The map file is imported into Zeiss Zen Black using a custom STOMP Macro. The STOMP Macro guides the 2-photon laser to selectively deliver UV energy to each SOI identified in the map, conjugating biotin-BP to any protein within the bounds of each SOI. **E**, Biotinylated SOI proteins are affinity-purified using streptavidin-coated beads and identified by liquid chromatography-mass spectrometry (LC-MS). Both stained (red) and unstained (black) proteins within the SOI are biotinylated. **F**, Slides are mounted in a media containing a bi-functional, biotin-benzophenone (biotin-BP) affinity purification tag that is activated by UV to covalently attach to local carbon or nitrogen. **G**, To automate STOMP (auto-STOMP) a tile array of each field of view across the sample is generated using a custom python script and Zeiss Zen Black coordinate functions. **H**, The SikuliX icon recognition software is used to automate the basic STOMP protocol (auto-STOMP) by integrating the directed network of tasks between Zen Black (autofocus and image acquisition (B) and map guided photo-labeling(C)) and Fiji (image processing and map generation(D)). **I**, Instant messages are delivered to the user through Gmail portal for the update of automation status (Success/Failure/Frozen). Red boxes indicate auto-STOMP protocol updates.

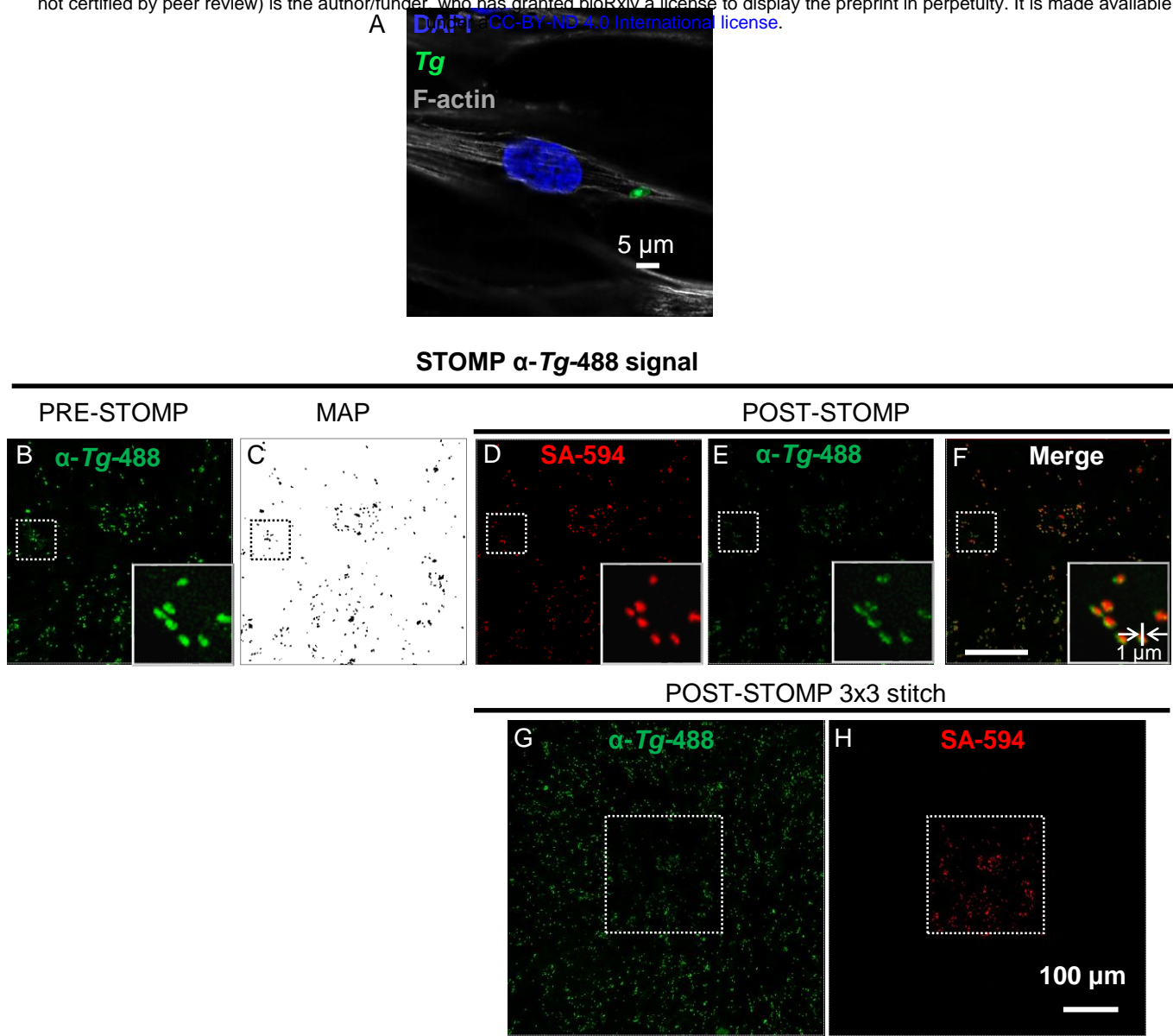


Figure 2. Structure of interest (SOI) proteins are selectively biotinylated by autoSTOMP UV-cross linking. **A**, Representative image of a GFP-expressing strain of *Toxoplasma* (*Tg*) infecting a human foreskin fibroblast (HFF), nuclei stained with DAPI, F-actin stained with phalloidin-660 after PFA fixation. **B**, Methanol fixed *Tg* infected HFFs were stained with a *Tg*-specific antibody directly conjugated to Alexafluor-488 (α -Tg-488, green) to identify *Tg* as the SOI. **C**, The MAP file generated in FIJI identifying the *Toxoplasma* SOI imaged in **B**. **D-F**, After UV-mediated biotin-BP tagging, biotinylated proteins were visualized using streptavidin-Alexafluor594 staining (**D**, SA-594, red), and directly compared to the *Tg* signal (**E**, α -Tg-488, green). Note photobleaching due to UV-targeting. **F**, merge of **D** and **E**. **G-H**, 3x3 tile array centered on the field of view targeted by the STOMP macro (white dotted line box): *Tg* staining (**G**, α -Tg-488, green) and biotinylation (**H**, SA-594, red). Representative of 3 independent experiments.

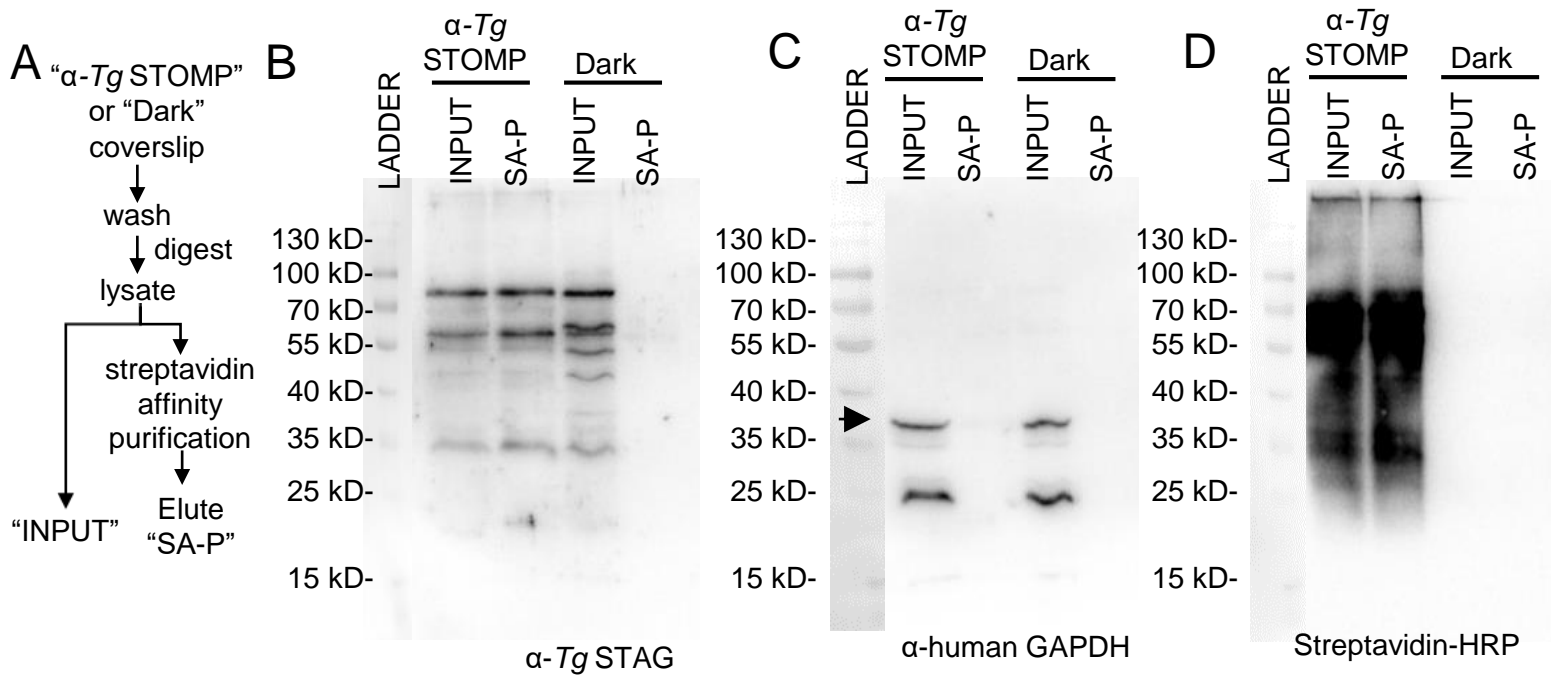


Figure 3. Structures of interest (SOI) proteins are enriched by autoSTOMP mediated-biotinylation and streptavidin (SA) precipitation. **A**, Schematic of the precipitation procedure. **A-D**, *Toxoplasma gondii* (*Tg*) infected human foreskin fibroblasts (HFFs) were stained with an α -*Tg488* antibody to identify SOI for auto-STOMP (α -*Tg* STOMP) as described in Figure 2. Alternatively, samples that have been treated identically but not exposed to UV light (Dark) serve as a control for background biotinylation and/or non-specific binding to SA-beads. Following UV crosslinking coverslips are washed to remove excess unconjugated biotin-BP, digested in 8 M urea lysis buffer and split in half. One half is reserved as the input loading control (INPUT). In the other half, biotinylated proteins are enriched by streptavidin (SA) bead precipitation. Following precipitation, samples are washed extensively and eluted in SDS Page loading dye by boiling “SA-P”. **B**, *Tg* proteins are enriched in the α -*Tg* STOMP sample relative to the Dark control when α -*Tg488* is used to identify SOI. Note, antibody detects multiple *Tg* proteins. **C**, Human GAPDH (arrow heads) is not enriched by STOMP when α -*Tg488* is used as a SOI. **D**, Biotinylated proteins are enriched in STOMP samples relative to input and Dark controls. Representative of 3 independent experiments.

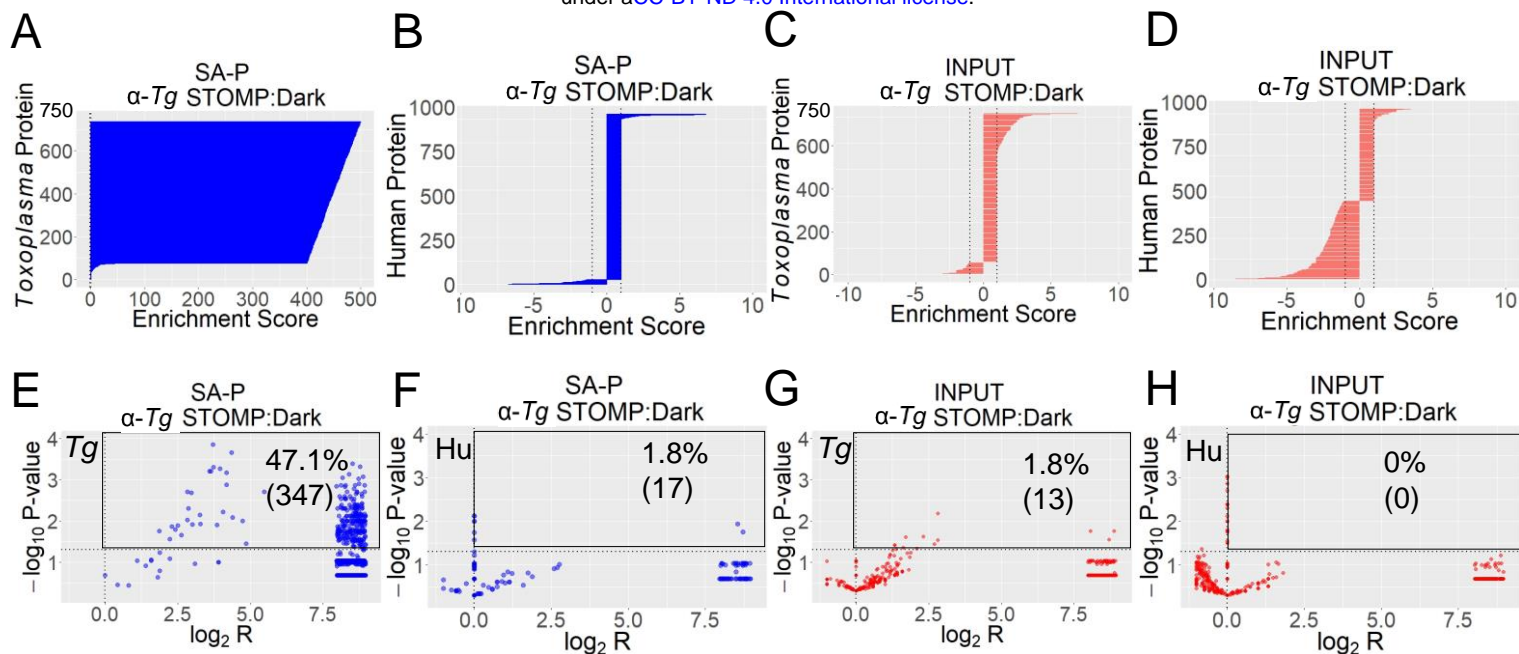


Figure 4. Structure of interest (SOI) proteins are enriched by peptide sequencing using auto-STOMP. *Toxoplasma gondii* (Tg) infected human foreskin fibroblast (HFF) were biotinylated and precipitated as described in Figure 3 including Tg SOI biotinylated by autoSTOMP (α -Tg STOMP) or identical samples not exposed to UV-light (Dark control). Streptavidin precipitate (SA-P) samples were on-bead digested with trypsin/lysC and the input controls (INPUT) were trypsin digested. 736 Tg proteins and 960 human proteins were detected with FDR < 1% for peptide and protein identification. **A-D**, Tg proteins were enriched in α -Tg STOMP SA-P samples relative to the Dark SA-P controls (**A**) whereas human proteins were not enriched (**B**). Neither Tg proteins (**C**) or human proteins (**D**) were enriched in the α -Tg STOMP INPUT samples relative to dark INPUT controls. A positive enrichment score represents the spectral count ratio (SCR) of α -Tg STOMP over Dark; a negative enrichment score represents the negative inverse SCR ($-1/SCR$) of α -Tg STOMP over Dark. Lines represent enrichment score of -1 and 1 . **E-H**, Volcano plots representing the significance ($-\log_{10} P$ value) versus fold enrichment (\log_2 of SCR) in α -Tg STOMP samples relative to Dark control samples. A majority of Tg proteins identified are significantly enriched in α -Tg STOMP SA-P samples relative to Dark SA-IP (**E**, black square, significant enrichment with $P < 0.05$, $n=3$) whereas human proteins are not significantly enriched (**F**). Neither Tg proteins (**G**) or human proteins (**H**) are significantly enriched in α -Tg INPUT samples relative to Dark INPUT samples. Each dot presents a protein. Dotted lines represent $y = -\log_{10} 0.05$ (significant enrichment, $P < 0.05$, $n = 3$) and $x = 0$ (no fold change). P-value represents student's t test comparing each pair of samples across three independent experiments. All proteins are listed in Table S-1.

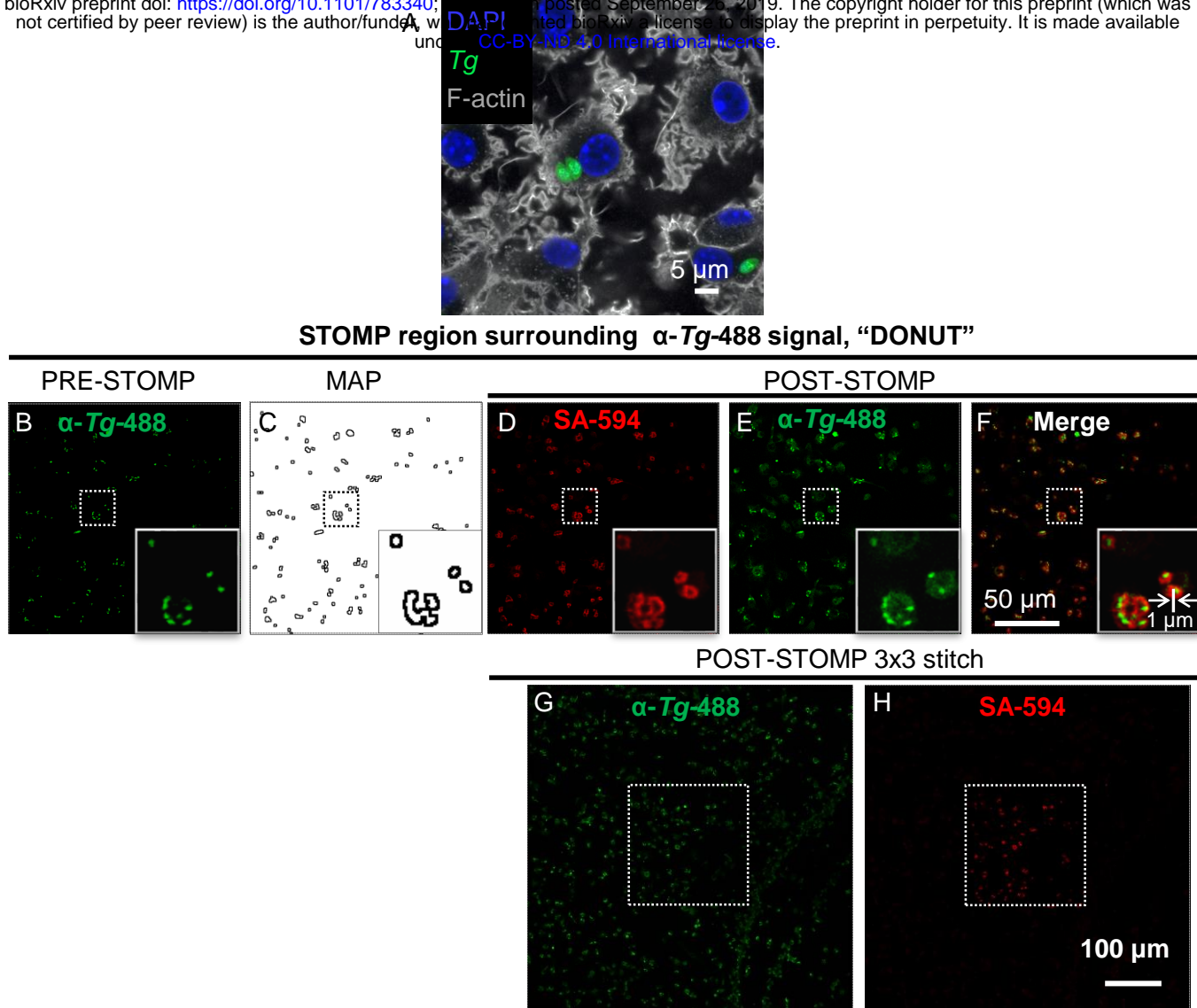


Figure 5. AutoSTOMP selectively biotinylates custom structure of interest (SOI) proteins. **A**, Representative image of a GFP-expressing strain of *Toxoplasma* (*Tg*) in infected mouse bone marrow derived dendritic cells (mBMDCs). Nuclei stained with DAPI and F-actin stained with phalloidin-660 after PFA fixation. **B**, Methanol fixed *Tg* infected mBMDCs were stained with a *Tg*-specific antibody directly conjugated to alexafluor-488 (α -*Tg*-488, Green) to identify *Tg*. **C**, The MAP file generated in FIJI identifying the 2 pixels surrounding but excluding the *Tg* as the SOI (DONUT). **D-F**, After UV-mediated biotin-BP tagging, biotinylated proteins were visualized using streptavidin-Alexafluor594 staining (**D** SA-594, red), and directly compared to the *Tg* signal (**E**, α -*Tg*-488, green); **F**, merge of **D** & **E**. Inset is an enlarged view of the dotted line box. **G-H**, 3x3 tile array around the STOMP targeted field of view (white dotted line box): *Tg* staining (**G**, α -*Tg*-488, green) or biotinylation (**H**, SA-594, red). Representative of 3 independent experiments.

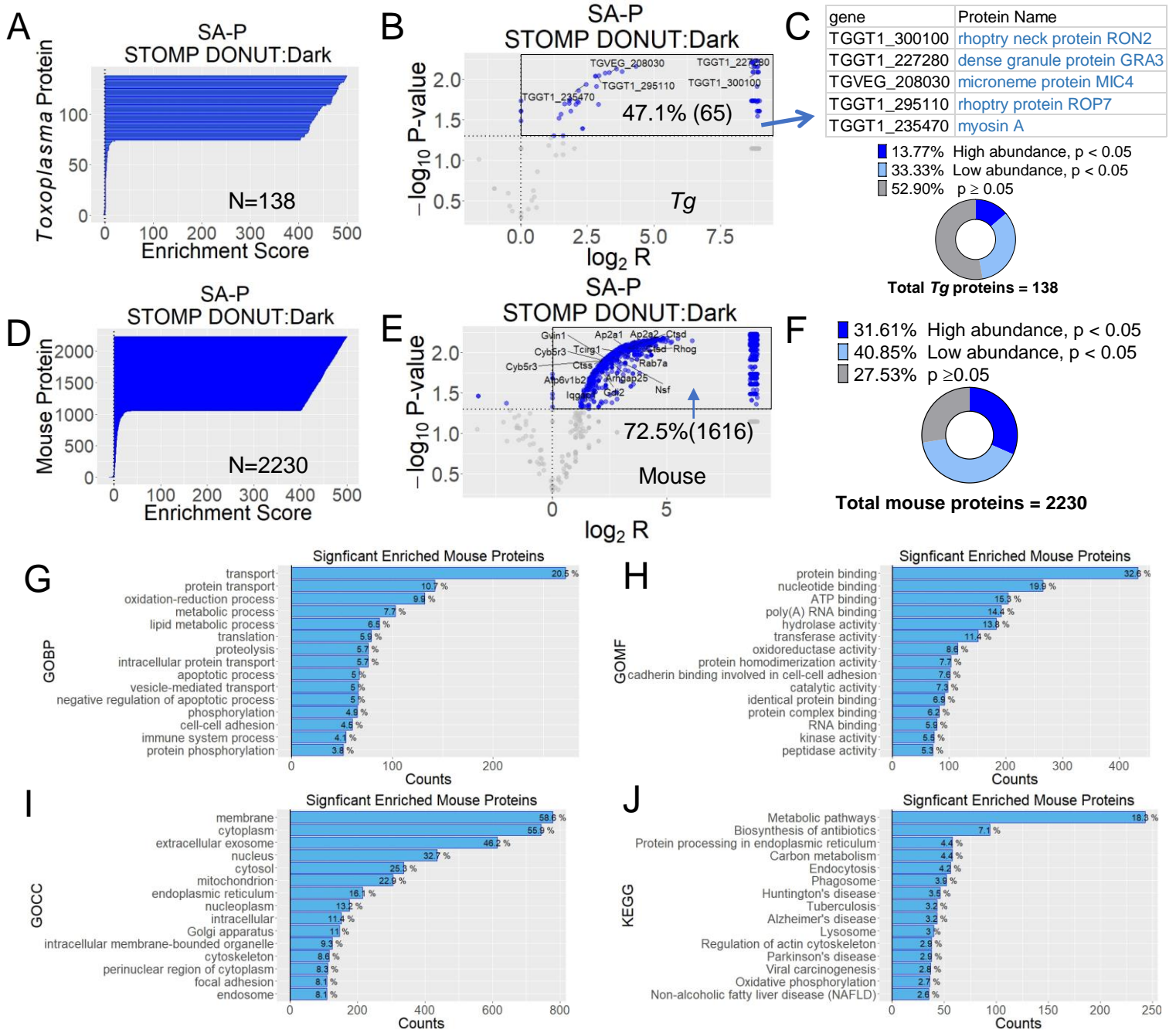
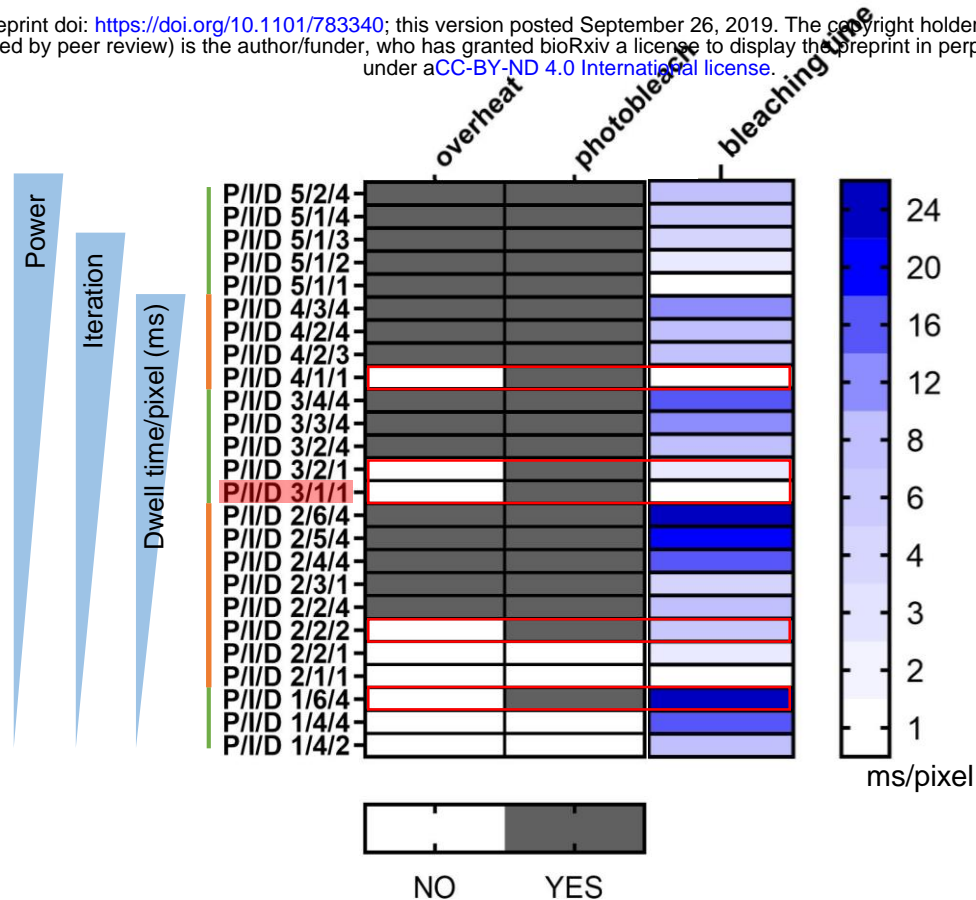


Figure 6. Legend in the next page.

Figure 6. AutoSTOMP selectively identifies host and parasite proteins in custom SOI surrounding *Tg*. The regions surrounding but excluding *Toxoplasma gondii* (*Tg*) (STOMP DONUT) in mouse bone marrow derived dendritic cells (mBMDCs) were identified as SOI using the autoSTOMP 'donut macro' and biotinylated as described in Figure 5. STOMP DONUT and identical samples not exposed to UV-light (Dark) were purified by streptavidin precipitated (SA-P) and on-bead digested for LC-MS. 138 *Tg* proteins and 2230 mouse proteins were detected with FDR < 0.2% of peptide identification and FDR < 2% of protein identification. P-values are calculated from the Student's t-test between the three replicates of STOMP DONUT SA-P sample and Dark SA-P sample (significant difference, $p < 0.05$; no significant difference, $p \geq 0.05$). The proteins in STOMP DONUT SA-P sample with spectral counts ≥ 5 are annotated as "high abundance" whereas those with spectral counts < 5 are annotated as "low abundance". **A-C**, Of the 138 *Tg* proteins detected in the STOMP DONUT SA-P samples relative to the Dark SA-P samples (**A**), 47.1% or 65 *Tg* proteins were significantly enriched (**B**, blue dots). Confirmed PVM-localized proteins are indicated by their gene code and annotated in the table below. **C**, The 138 *Tg* proteins grouped by p-value and abundance. **D-F**, Of the 2230 mouse proteins enriched in the STOMP DONUT SA-P samples relative to the Dark SA-P samples (**D**), 72.5% or 1616 were significantly enriched, (**E**, blue dots). A selection of host PVM associated proteins are annotated by gene name. **F**, The 2230 *Tg* proteins grouped by p-value and abundance. **A&D**, A positive enrichment score represents the spectral count ratio (SCR) of STOMP DONUT over Dark; a negative enrichment score represents the negative inverse SCR ($-1/SCR$) of STOMP DONUT over Dark. **B&E** Volcano plots show the significance ($-\log_{10} P$ value, $n = 3$) versus fold enrichment (\log_2 of SCR, mean of three replicates) in STOMP DONUT samples relative to Dark samples. Blue indicates $p < 0.05$, or gray indicates $p \geq 0.05$. Black box indicates proteins significantly enriched by autoSTOMP. **C&F**, Proteins enriched in the STOMP DONUT sample relative to the Dark control are categorized by p-values and spectral counts above ≥ 5 (high abundance) or below < 5 (low abundance) represented as pie charts. $N = 3$ independent experiments. **G-J**, The 72.5% or 1616 significantly enriched mouse proteins (**E**) are plotted with the Gene Ontology (GO) terms or KEGG terms against the counts of the proteins involved. Three types of (GO) terms (Biological Process (BP, **G**), Molecular Function (MF, **H**), or Cellular Component (CC, **I**) or KEGG pathway terms (**J**) are used. The terms are ranked by the counts from the largest to the smallest and annotated with the percentage of involved proteins out of the total. Here, only the top 15 terms are shown.

A



B

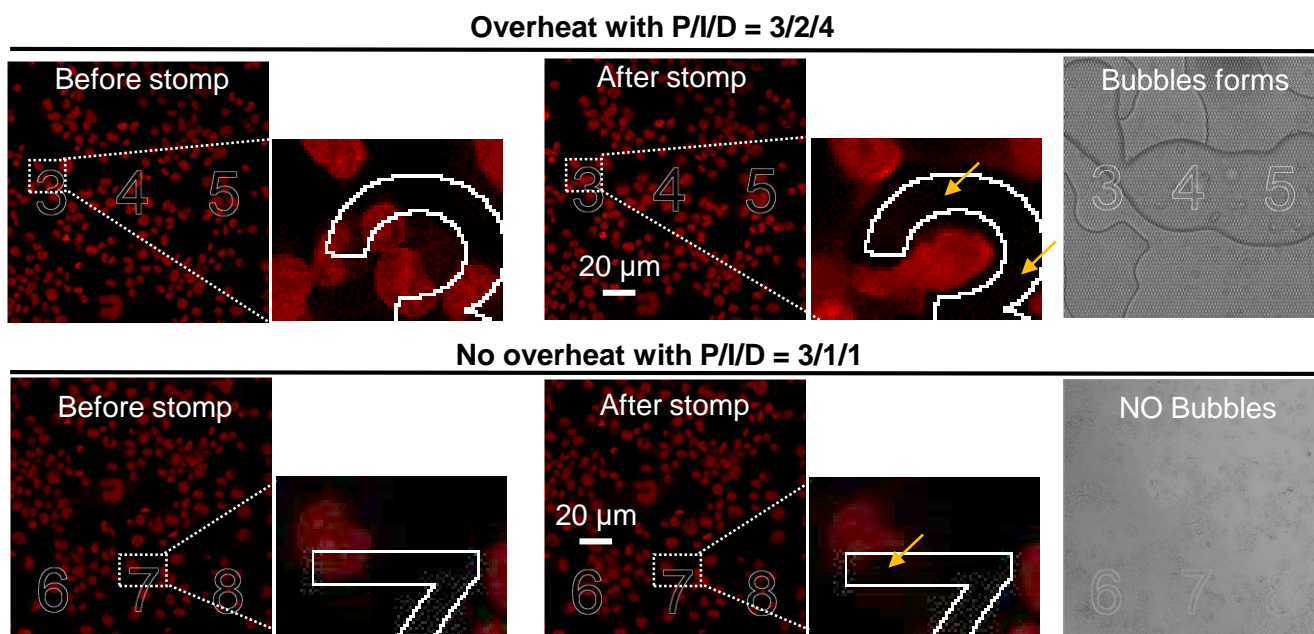


Figure S-1 The optimal photo-crosslinking condition was determined varying the laser power (P), the number of iterations each field of view was photo-excited (I) and the dwell time (D) represented as “P/I/D” using methanol fixed THP-1 cells stained with propidium iodide. **A**, Five conditions were identified with sufficient power for photo-bleaching that did not induce overheating (red box). P/I/D = 3/1/1 was chosen to minimize the time necessary to process each field of view. Samples are primarily ordered by the power (P), secondly ordered by the iteration time (I) and thirdly ordered by the Dwell time/pixel (ms). The bleaching time per pixel in milliseconds (ms) to excite the photo-crosslinking equals the product of the iteration time and Dwell time/pixel. **B**, Representative laser settings for photo-crosslinking that causes the overheating with P/I/D = 3/2/4 (Top) or no overheating with P/I/D = 3/1/1 (Bottom) inside the slide. The STOMP crosslinking was directed to the SOIs with the shapes of numbers “3”, “4”, and “5” (Top) or numbers “6”, “7”, “8” (Bottom). The photobleaching occurs in the auto-STOMP targeted SOIs (yellow arrow) while the outside area was not affected (outside the white outline). Bubbles formed were detected under the bright field indicating overheating.

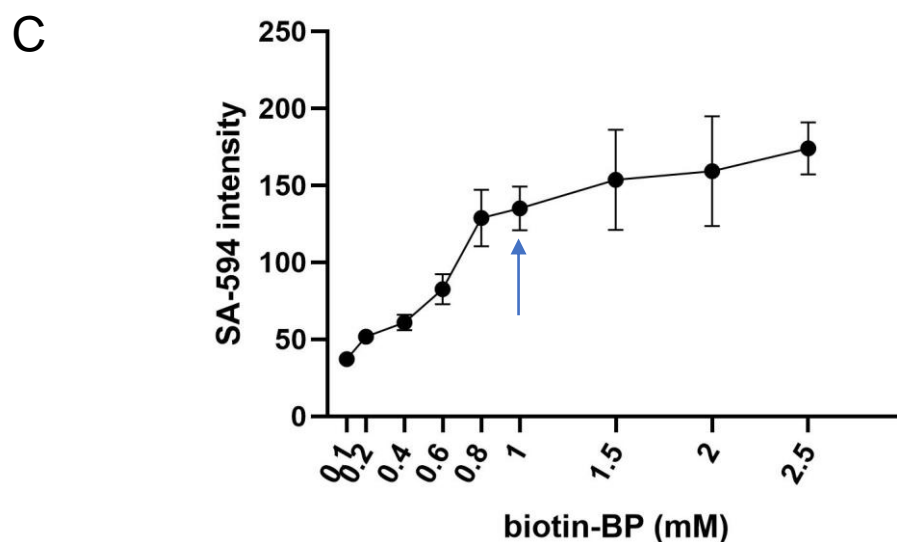
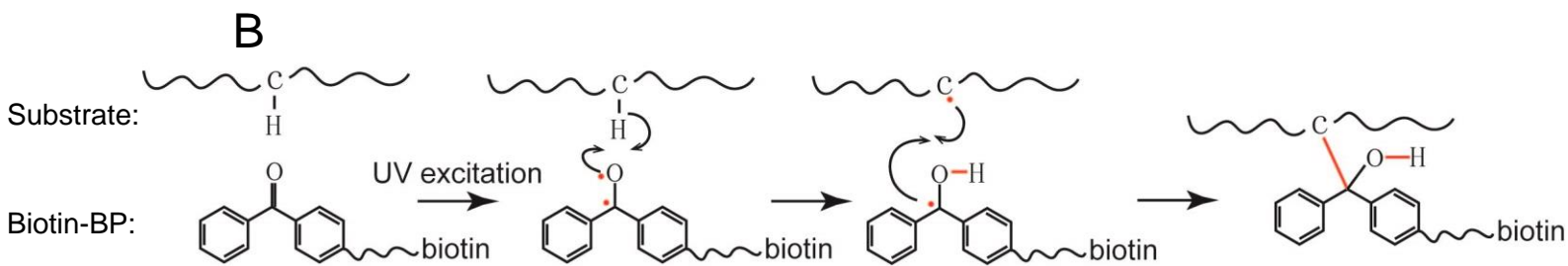
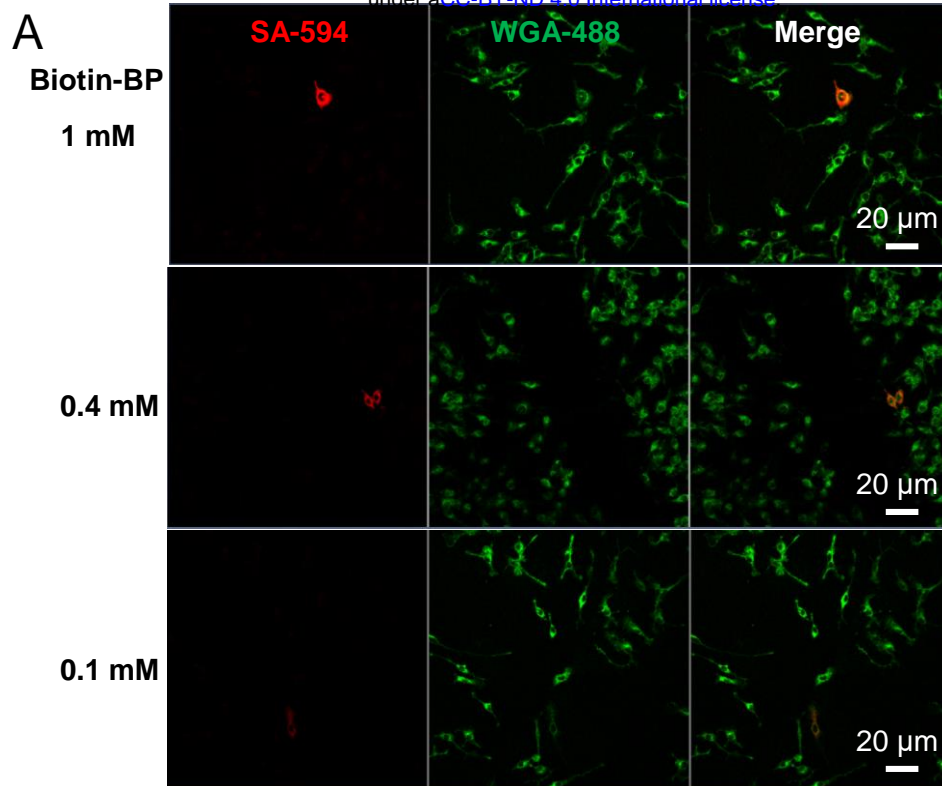


Figure S-2. Biotin-BP concentration was optimized by titration 0.1mM to 2.5mM biotin-BP in mounting media. Immortalized mouse bone marrow derived macrophages (iBMDMs) were methanol fixed and stained with fluorescein labeled wheat germ agglutinin (WGA-488) then mounted with biotin-BP at concentrations of 0.1 – 2.5 mM. Samples were photo-crosslinked at 720 nm at laser Power/Iteration/Dwell time = 3/1/1. **A**, Representative images of iBMDMs (green) and 0.1, 0.4 and 1mM biotin-BP showing an individual cell targeted with streptavidin-594 (red). **B**, A diagram shows biotin-BP inserts into C-H or N-H bonds under UV. **C**, SA-HRP staining relative to biotin-BP concentration. 1mM biotin-BP (blue arrow) was selected as the lowest concentration needed for optimal SA-594 staining.

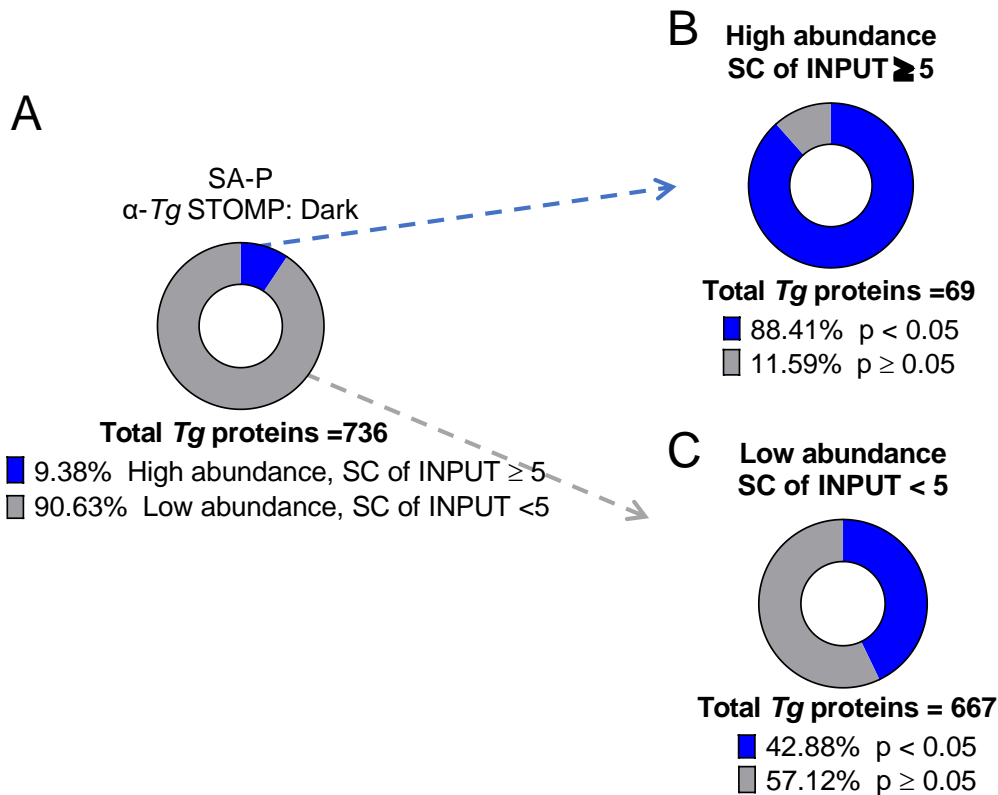


Figure S-3. Both high and low abundance proteins are enriched by autoSTOMP. **A**, Of the 736 *Toxoplasma gondii* (*Tg*) proteins identified in Figure 4E, 9.38% of proteins are “high abundance” with spectral counts (SC) in the INPUT controls \geq 5, and 90.63% of proteins were “low abundance” with SC in the INPUT controls < 5. p-values based on student’s t-test comparing α -Tg STOMP SA-P and Dark SA-P samples. N=3 independent experiments (significant difference, $p < 0.05$; no significant difference, $p \geq 0.05$). **B**, 88.41% of the high abundance proteins are significantly enriched by autoSTOMP. **C**, Whereas, 42.88% of the low abundance proteins are enriched in the α -Tg STOMP compared to the Dark.

STOMP α -Tg-488 signal

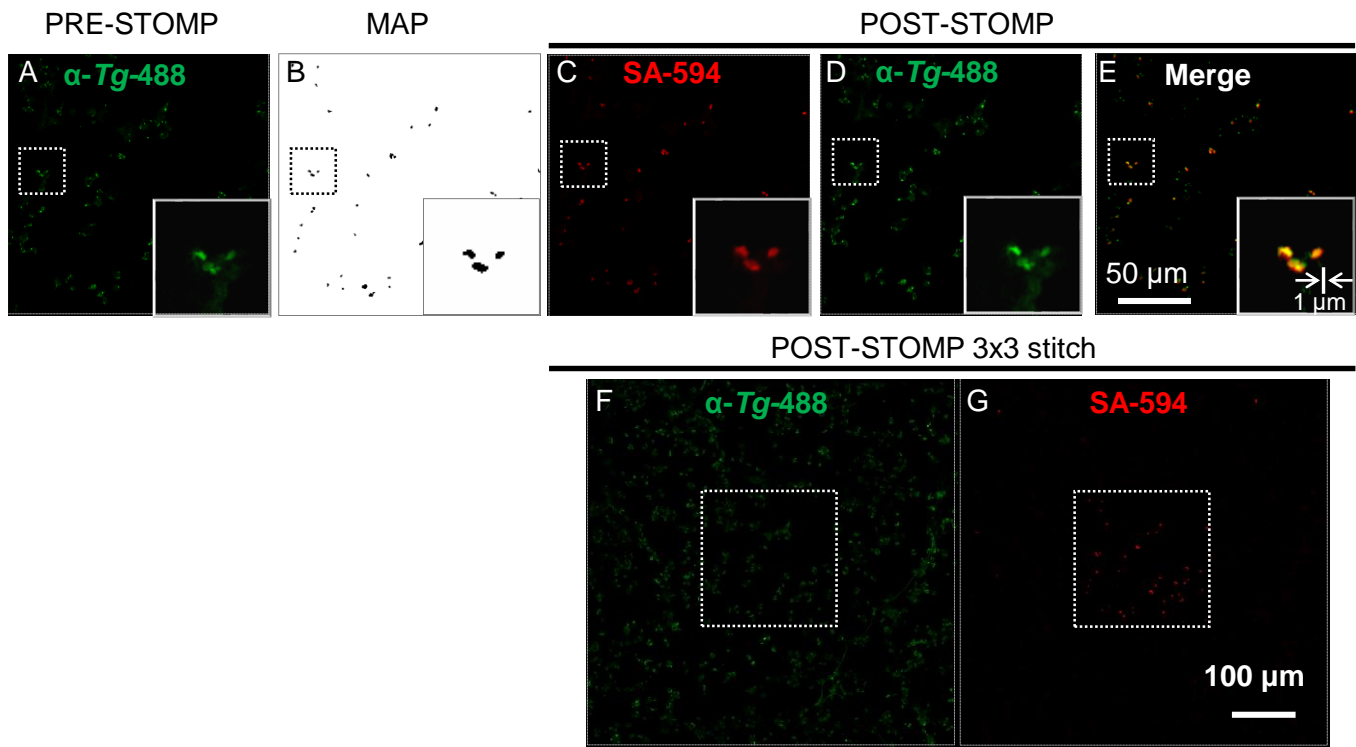


Figure S-4. The *Tg* is selectively biotinylated by auto-STOMP UV-cross linking in *Toxoplasma* (*Tg*) infected mouse bone marrow derived dendritic cells (mBMDCs). **A**, *Tg* in mBMDCs were stained with a *Toxoplasma*-specific antibody directly conjugated to alexafluor-488 (α -*Tg*-488, green) to identify *Tg* as the SOI. **B**, The MAP file generated in FIJI identifying the *Tg* SOI imaged in **A**. **C-E**, After UV-mediated biotin-BP tagging, biotinylated proteins were visualized using streptavidin-Alexafluor594 staining (**C**, SA-594, red), and directly compared to the *Tg* signal (**D**, α -*Tg*-488, green). **E**, merge of **C** and **D**. **F-G**, 3x3 tile array centered on the field of view targeted by the STOMP macro (white dotted line box): *Toxoplasma* staining (**F**, α -*Tg*-488, green) and biotinylation (**G**, SA-594, red). Representative of 3 independent experiments.